

13. PLEISTOCENE CALCAREOUS NANNOFOSSIL BIOSTRATIGRAPHY AND THE WESTERN MEDITERRANEAN SAPROPELS, SITES 974 TO 977 AND 979¹

Eric de Kaenel,² William G. Siesser,³ and Anne Murat⁴

ABSTRACT

During Ocean Drilling Program Leg 161, six sites were drilled in the western Mediterranean. Pleistocene sediments were cored at Sites 974, 975, 976, 977, and 979. Occurrences of generally very abundant and well-preserved calcareous nannofossils provide a new Pleistocene biostratigraphic framework based on a succession of twenty biohorizons. Calibration of these datums with the orbital time scale, based on the average of June and July (summer) insolation time series at 65°N of the astronomical solution La90_(1,1), gives the following ages in Ma: (FO, first occurrence) *Emiliania huxleyi* >*Gephyrocapsa* spp. (0.070); (FcO, first consistent occurrence) *E. huxleyi* (0.218); (FO) *E. huxleyi* (0.270); (LO, last occurrence) *Pseudoemiliania lacunosa* (0.406); (LO) *P. lacunosa lacunosa* (>7 μm) (0.439); (LO acme) *P. lacunosa* (0.739); (LO) *Crenalithus asanoi* (cir.; >6.5 μm) (0.781); (FO) *Gephyrocapsa omega* (>4) (0.962); (FO) *C. asanoi* (circular; >6.5 μm) (1.122); (LO) *Gephyrocapsa* spp. (>6.5 μm) (1.235); (LO) *Helicosphaera sellii* (1.246); (LcO, last consistent occurrence) *H. sellii* (1.276); (FO acme) *P. lacunosa* (1.361); (FO) *Gephyrocapsa oceanica* (>6.5 μm) (1.494); (FO) *Gephyrocapsa caribbeanica* (>6.5 μm)-*G. oceanica* (>6.3 μm) (1.525); (FO) *G. oceanica* (>5.5 μm) (1.566); (FO) *Gephyrocapsa* spp. (>5 μm) (1.615); (LO) *Calcidiscus macintyreii* (cir.; >11 μm) (1.619); (FO) *G. oceanica* (>4) (1.719); (FO) *G. caribbeanica* (>4) (1.726).

Sapropels (organic-rich layers) interlayered in pelagic and hemipelagic Pleistocene sediments recorded at each western Mediterranean site are calibrated with the orbital time scale and numbered following the codification of the insolation cycles. Sixty-eight insolation cycles were recognized in these Pleistocene sediments from a total of 88 insolation cycles for the Pleistocene (= 176 insolation minima and maxima). The western Mediterranean Sites 974–979 represent sections with continuous sapropel records that span the entire Pleistocene and indicate that the temporal sapropel pattern is not evenly distributed. The calibration of the western Mediterranean sapropels to the orbital time scale and to the oxygen isotope stratigraphy provides precise stratigraphic correspondence that will be used to compare the timing of eastern and western Mediterranean sapropel cyclicity.

Four new combinations are also introduced: *Crenalithus asanoi*, *Crenalithus japonicus*, *Pseudoemiliania pacifica*, and *Pseudoemiliania lacunosa ovata*.

INTRODUCTION

The present work is based on the study of five Ocean Drilling Program (ODP) sites drilled in the western Mediterranean from the Tyrrhenian Sea (Site 974), the South Balearic Sea (Site 975), to the Alboran Sea (Sites 976, 977, and 979). Based on characteristics of the sediments recorded by visual core descriptions (principally color criteria), photographs, and total organic carbon (TOC), a number of sapropels were described and coded for each site (Comas, Zahn, Klaus, et al., 1996; Murat, Chap. 41, this volume). TOC content found in sapropels at Leg 161 sites displays a wide range of values, from 0.7% to more than 6% (Comas, Zahn, Klaus, et al., 1996; Murat, Chap. 41, this volume).

Recent works from Hilgen (1991) and Lourens et al. (1994, 1996a, 1996b) have demonstrated that the occurrences of sapropels correlate with minima in the Earth's orbital precession cycle. This cyclicity occurs with an average of 20,700 yr. During the periods of minima in the Earth's orbital precession, the northern hemisphere receives stronger summer insolation and weaker winter insolation than it receives at present. This implies that the insolation variation at the Earth's surface may be derived from its precession cycles. Generally, the phase lags between precession cycles, and their induced climatic

variations are assumed constant (Lourens et al., 1996a). A time lag of 3 k.y. is used in this study, following Lourens et al. (1996a), between the age of the insolation peak and the age of the climatic response. The astronomical calibration of the insolation parameters used in this study is from the astronomical solution, La90_(1,1), corrected for dynamical ellipticity and tidal dissipation, calculated by Laskar et al. (1993). Astronomical calibration of individual sapropels are derived from the insolation parameter with a time lag of 3 k.y. and minima and maxima of cycles are coded (*i* = insolation) from the present. Odd numbers correspond to maxima and even numbers to minima in the insolation curve. Astronomical calibration of the sapropels was established at Sites 975, 976, and 977 based on biochronology and on correlations to the oxygen isotope records. A high-resolution biochronological framework established at these sites, together with sapropel distribution patterns, were used to calibrate the sapropels described at Sites 974 and 979.

Based on shipboard analyses during Leg 161 and on detailed sapropel study, a coding with Key Bed Number of sapropels is presented by Murat (Chap. 41, this volume). The number of cycles, identified in late Pliocene–Pleistocene sediments, varies from site to site: 33 at Site 974, 32 at Site 975, 28 at Site 976, 42 at Site 977, and 45 at Site 979. Based on the stratigraphic analyses of the five sites, the total Pleistocene sapropels recorded represent 68 insolation cycles (from 88 cycles). Eighteen “missing cycles” (*i* = 14, 28, 32, 34, 36, 42, 76, 78, 106, 114, 120, 146, 150, 154, 158, 162, 164, and 174) correspond to periods with low maxima peaks in the insolation curve. During these periods of weak insolation variations, no sapropels were developed in the sediments. The other two “missing sapropels” are the insolation peaks *i* = 26 and 118. Five insolation cycles (*i* = 178, 180, 182, 188, and 208) were described in the uppermost Pliocene intervals recorded at Sites 974 and 979. The Pliocene/Pleistocene bound-

¹Zahn, R., Comas, M.C., and Klaus, A. (Eds.), 1999. *Proc. ODP, Sci. Results*, 161: College Station, TX (Ocean Drilling Program).

²Florida State University, Department of Geology, B-160, Tallahassee, FL 32306, U.S.A. (Present address: Institut de Géologie, Université de Neuchâtel, Rue Emile-Argand 11, 2000 Neuchâtel, Switzerland.) edekaenel@bluewin.ch

³Department of Geology, Box 46-B, Vanderbilt University, Nashville, TN 37235, U.S.A.

⁴INTECHMER, BP 324, Cherbourg Cedex, France.

ary has been correlated with the top of i-cycle 176 at the type section from Vrica (Italy) by Hilgen (1991) and an age of 1.806 Ma determined. The Pleistocene contains 176 maxima and minima, or 88 cycles. Most of the peaks in the insolation curve correspond with the occurrence of sapropels. However, most of the cycles are represented in the sediments in the Mediterranean by the development of redox cycles (Murat, 1991; Murat, Chap. 41, this volume).

Derived from the astronomical calibration of sedimentary cycles, a Pleistocene astronomical time scale has been constructed by Hilgen (1991) and Lourens et al. (1996a), based on the correlation of sapropel and carbonate cycle patterns to the precession cycles. Uppermost Pleistocene sapropels (i-cycles 2 to 46) found in the eastern Mediterranean were first numbered by Cita et al. (1977) and later calibrated to the insolation peak (Hilgen, 1991). Lower Pleistocene sapropels (i-cycles 124 to 176) from outcrop sections in Italy were used to develop the astronomical time scale (Hilgen, 1991; Lourens, 1994). At the same time, seven calcareous nannofossil datums were calibrated to the insolation peaks and ages derived from their stratigraphic positions (Hilgen, 1991; Lourens et al., 1996a). Additionally, Castradori (1993), studying a set of eastern Mediterranean deep-sea cores, calibrated five calcareous nannofossil datums based on sapropel layers, isotopic records, and magnetostratigraphy. The western Mediterranean Sites 974 to 979 contain Pleistocene sections with sapropel records from the lowermost to the uppermost Pleistocene. By calibration of the sapropels with the insolation peaks, we calculated more precise ages for 20 calcareous nannofossil events. Of the 20 datums, four are new events: the beginning of the acme of *Pseudoemiliana lacunosa* (1.361 Ma), the end of the acme of *Pseudoemiliana lacunosa* (0.739 Ma), the LO of *Pseudoemiliana lacunosa* (>7 µm) (0.439 Ma), and the first consistent occurrence of *Emiliana huxleyi* (0.218 Ma). Among the other calcareous nannofossil events, some datums, such as the LO of *Pseudoemiliana lacunosa* (0.406), differ from the generally accepted ages.

METHODS

In order to obtain good-quality slides, all samples used in this study were prepared using a settling technique. Approximately 2000 samples were processed and at least three samples were examined from each core section. The published literature describes different settling techniques, mainly for preparing samples for scanning electron microscope (SEM) studies. These settling techniques are used to eliminate particles with a size range <2 µm and >30 µm. In this study, the settling technique used to prepare slides for the light microscope follows the procedure described by de Kaenel and Villa (1996).

Semiquantitative measurements were used to place first and last occurrences, as well as changes in abundances of taxa. For some acme events, the number of specimens per field of view was also recorded.

As in many morphometric studies, detailed observations in the microscope are necessary to determine accurately FOs based on size. Our work, based on five different holes with Pleistocene records documented the stratigraphic position of several morphometric changes. The results at one hole will either corroborate or modify the interpretations in all the other holes. If a new biostratigraphic position was obtained in one hole, all other holes were re-examined to verify the position of the datums. This was done many times during this study, especially to locate the *Gephyrocapsa* events based on size changes. As for many morphologic changes, only very rare specimens in the *Gephyrocapsa* populations have the new character. Thus, the stratigraphic position of the FO of a particular *Gephyrocapsa* morphotype is often based on the observation of one or two specimens, but is also dependent on the sampling resolution. Without frequent sampling, the precise positioning of a datum is not possible.

Using these datums as reference points, the age-depth relationships were plotted. Additionally, the sapropel layers were plotted with the nannofossil datums according to their depth and with an estimated astronomical age (Table 1) according to sapropel patterns and characteristics:

1. Distinct sapropels with high TOC content are assumed to be directly related to high-amplitude insolation maxima and less distinct sapropels with low TOC content are assumed to be related to low-amplitude insolation maxima (Lourens et al., 1996a).
2. As important are the thick-thin-thick alternation of sapropels in a short time interval (small-scale sapropel clusters). In land sections, they correspond to an alternation of high-low-high amplitude precession minima (Lourens et al., 1996a).
3. Intervals containing more and thicker sapropels correspond to the large-scale sapropel clusters described in land sections by Hilgen (1991).

In a second step, the new nannofossil datums were introduced in the age-depth plot, and precise ages for the 20 datums were established by their depth position between the two closest sapropels. The ultimate chronological precision of a datum depends on the sample resolution and on the precise determination of the position of tops and bottoms of the sapropels. Based on these criteria, a best estimate of the datum age was selected from the five sites studied. They are proposed as new standards for Pleistocene biostratigraphic framework.

Table 1. Insolation cycle (i-cycle) ages.

Insolation cycles (i-cycle)	Age (ka)	Insolation cycles (i-cycle)	Age (ka)	Insolation cycles (i-cycle)	Age (ka)
2	8	88	934	174	1779
4	35	90	955	176	1808
6	55	92	976	178	1829
8	81	94	997	180	1851
10	102	96	1027	182	1872
12	124	98	1048	184	1900
14	148	100	1070	186	1923
16	172	102	1091	188	1944
18	195	104	1111	190	1965
20	217	106	1126	192	1982
22	240	108	1144	194	2000
24	262	110	1164	196	2020
26	288	112	1185	198	2040
28	310	114	1203	200	2059
30	331	116	1222	202	2071
32	353	118	1240	204	2094
34	369	120	1261	206	2115
36	385	122	1280	208	2137
38	405	124	1298	210	2160
40	425	126	1315		
42	444	128	1335		
44	461	130	1356		
46	483	132	1376		
48	503	134	1398		
50	528	136	1411		
52	553	138	1429		
54	575	140	1449		
56	597	142	1471		
58	618	144	1490		
60	647	146	1511		
62	668	148	1524		
64	690	150	1544		
66	710	152	1564		
68	732	154	1584		
70	747	156	1603		
72	765	158	1622		
74	785	160	1642		
76	804	162	1661		
78	822	164	1679		
80	841	166	1694		
82	862	168	1715		
84	882	170	1736		
86	908	172	1757		

Note: Ages correspond to the midpoints of the sapropels and are based on the astronomical solution La90_(1,1) of Laskar et al. (1993) with a time lag of 3 k.y.

Magnetostratigraphy records established on board are indicated for Sites 974 and 975 (see below, summary of sites), but were not used to calculate any datum ages. Many problems in determining the magnetic reversal boundaries were encountered on board ship because of uncertainties in the magnetic measurements.

Oxygen isotope records at Sites 975, 976, and 977 are not introduced in the age-depth plots, but the position of the nannofossil events within the $\delta^{18}\text{O}$ stages is indicated for each datum (see biohorizon descriptions below). Oxygen isotope records were also used to resolve discrepancies in sapropel stratigraphy. In few intervals, sapropels are not related to insolation maxima, but occur during insolation minima (see summary of Site 977 below).

RESULTS

Summary of Sites

Site 974

This site is located in the central Tyrrhenian Sea (Fig. 1), along the lower slope of the Sardinian continental margin in a small sub-basin more than 3400 m deep. At Site 974, four holes were drilled at about 3454 m water depth. This site lies about 300 m west-northwest of Site 652 (Leg 107). At Site 974, a complete Pleistocene sedimentary sequence was cored and 33 sapropels were identified, which were coded 401 to 433 (Fig. 2). The TOC maximal (TOC MAX) contents of these sapropels ranged from 0.9% to >6% (Comas, Zahn, Klaus, et al., 1996; Murat, Chap. 41, this volume). Calcareous nannofossils are very abundant at this site, and one interval contains a *Braarudosphaera bigelowii* (Br.) ooze (Fig. 2). High-resolution sampling and magnetostratigraphy provide a precise biostratigraphic framework to date the sapropels. The average sampling spacing for nannofossil analysis around and within the sapropels was 10 cm. The sapropels that were recognized at Site 974 were calibrated with the insolation cycles with a time lag of 3 k.y. and are presented in Figure 2. Some insolation cycles (Fig. 2; i-cycles 90, 92, and 122) are com-

posed of two sapropels, with generally one thin and one thick (e.g., i-cycles 92 and 122). Depths and characteristics of the sapropels are given by Murat (Chap. 41, this volume). The stratigraphic position of the datums according to the sapropels is presented in Figure 2 and discussed in the biohorizons section. The nannofossil events used to date the Pleistocene interval are listed in Tables 2 (depth) and 3 (estimated ages).

The magnetostratigraphy records at Site 974 are poorly defined except for Hole 974B; changes in inclinations in Holes 974A, 974C, and 974D were unclear as a result of secondary overprinting. In Hole 974B, the top of the Olduvai Chron (C1r.2r-2n/C2n boundary) is at 88.44 mcd (84.00 mbsf). This boundary is dated at 1.785 Ma by Lourens et al. (1996a) and lies in i-cycle 174. In Hole 974B, this boundary (Fig. 2) is between sapropel 429 (i-cycle 172 at 1.757 Ma) and sapropel 430 (i-cycle 176 at 1.808 Ma). The sapropel of i-cycle 174 is not distinct at Site 974, because of low TOC content (<0.5%). The same sapropel pattern is described on land sections in Italy (Vrica and Singa sections) by Hilgen (1991). Sapropels 433 to 426 correspond to the sapropel cluster "b-m" in Vrica. The Pliocene/Pleistocene boundary, situated at the top of the "e" sapropel in Vrica, is correlated with the top of sapropel 430 (i-cycle 176) in Hole 974C (89.995 mcd) and in Hole 974D (89.700 mcd). A position at 89.515 mcd is deduced for this boundary in Hole 974B, based on sapropel depths in Holes 974C and 974D. The age of i-cycle 176 is 1.808 Ma (Table 1) and the age of the Pliocene/Pleistocene boundary is estimated at 1.806 Ma by Lourens et al. (1996a). The FO of *Gephyrocapsa oceanica* (>4 μm) is situated between 86.55 and 86.37 mcd (best interpolated depth [BID] 86.46 mcd) and between sapropel 427 (i-cycle 168 at 1.715 Ma) at 86.24 mcd and sapropel 428 (i-cycle 170 at 1.736 Ma) at 87.04 mcd. The age for the datum at Site 974 is estimated at 1.721 Ma. The FO of *Gephyrocapsa oceanica* (>4) is situated at 3.05 m above the Pliocene/Pleistocene boundary and about 1.98 m above the top of the Olduvai Chron.

From sapropels 425 to 409, several small-scale clusters of two to seven sapropels are observed. The distinct cluster composed of sapropels 425 to 423 is correlated to the "n-p" cluster in Vrica. The

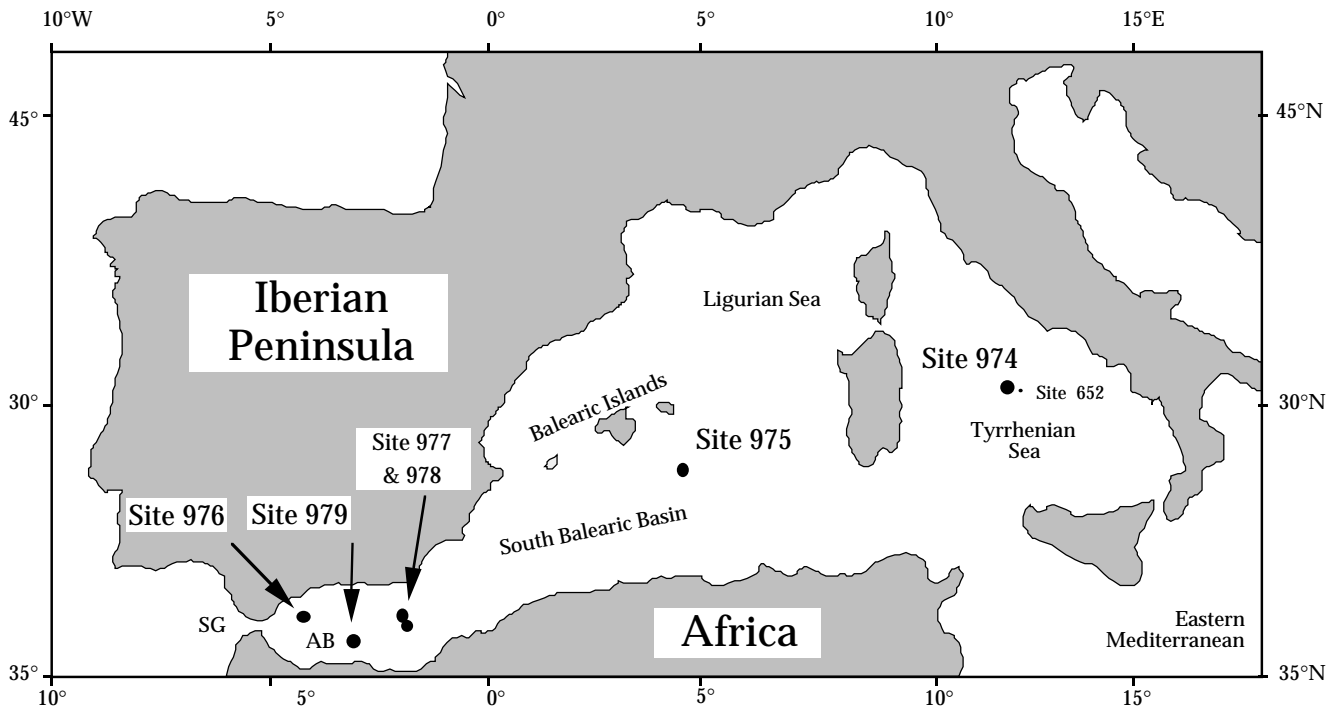


Figure 1. Location map of the western Mediterranean showing Leg 161 Sites 974–979 and Leg 107 Site 652. AB = Alboran Basin, SG = Strait of Gibraltar.

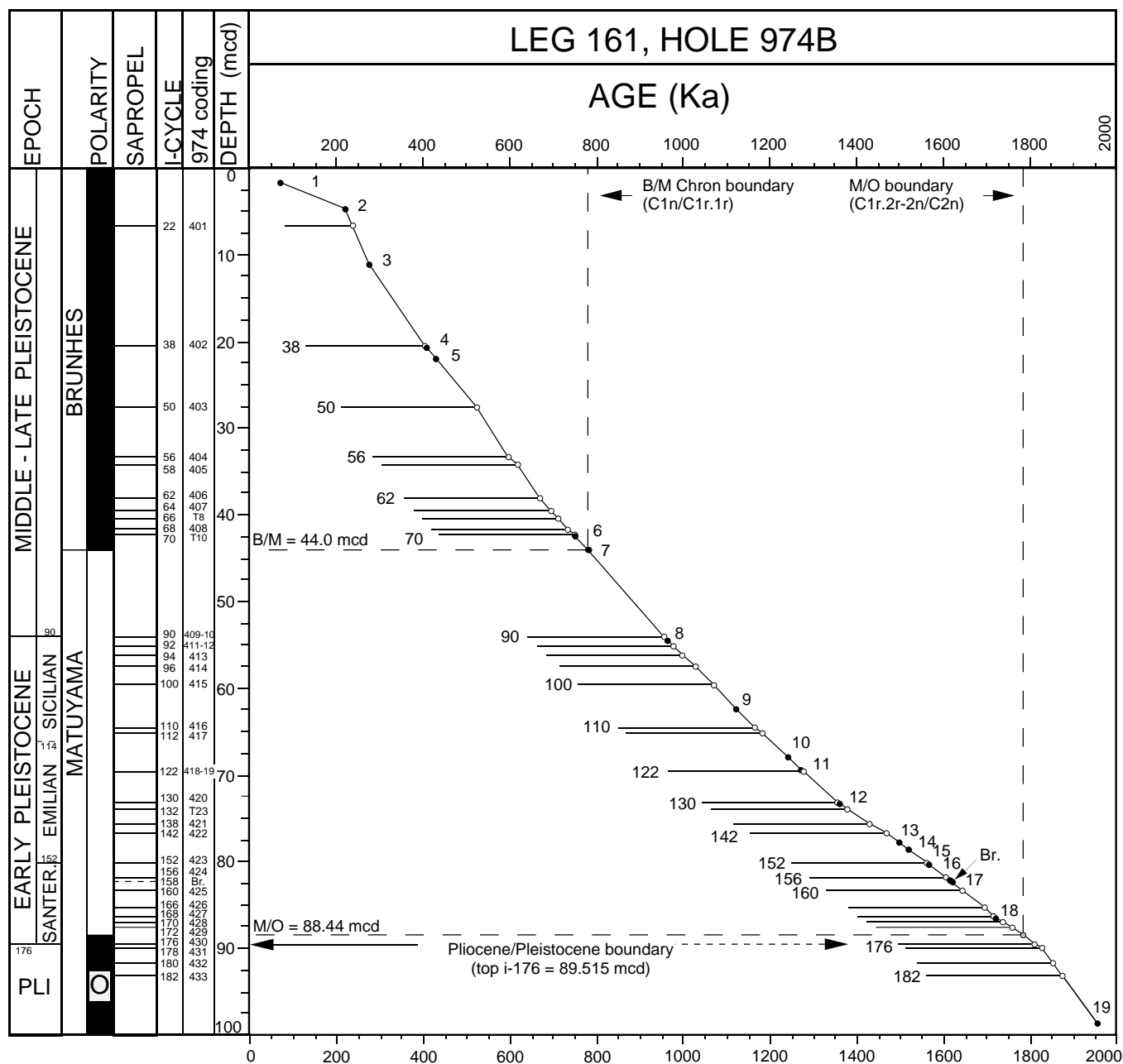


Figure 2. Age-depth plot. Calibration of sapropels in Hole 974B with the insolation cycles. Position and age of calcareous nannofossil events (19 black dots) are from Tables 2 and 3. Sapropels (34 white dots) are numbered (Site 974 coding described by Murat, Chap. 41, this volume) and correlated to the insolation cycle (i-cycle). Ages of i-cycles are indicated in Table 1. Br. = *Braarudosphaera bigelowii* bloom.

cluster composed of sapropels 422 to 418 corresponds to the “q-v” cluster in Vrica. The cluster of sapropels 415 to 409 is correlated to i-cycles 100 to 90.

Magnetostratigraphy records indicate that the B/M boundary (C1n/C1r.1r) is at 44.0 mcd in Hole 974B (Fig. 2). An age of 0.78 Ma for this boundary was calculated from astronomical calibration by Shackleton et al. (1990) at ODP Site 677 in the Equatorial Pacific. This age is between i-cycle 72 (0.765 Ma) and i-cycle 74 (0.785 Ma). Between i-cycle 90 (0.955 Ma) and i-cycle 70 (0.747 Ma), no sapropels were identified (Fig. 2). This interval represents a period of 0.208 k.y.

A small-scale cluster of sapropels (T10 to 406) is observed above the B/M boundary. This distinct sapropel alternation can be correlated to i-cycles 70 to 62. In the uppermost Pleistocene at Site 974,

sapropels are rare and only three insolation cycles are recorded: i-cycles 50, 38, and 22. When compared to the Late Pleistocene Mediterranean sapropel codification (S1 to S12) of Cita et al. (1977), i-cycle 38 corresponds to sapropel “S11” and i-cycle 22 to sapropel “S9” (Lourens et al., 1996a). Sapropel S1 to S8, and S10 were not recognized on board, but may still be discovered later with more detailed TOC analysis. At ODP Site 653 (Leg 107), located in the Tyrrhenian Sea to the west of Site 974, younger “S” sapropels were observed: S7 (i-cycle 18), S8 (i-cycle 20), S10 (i-cycle 30), and S12 (i-cycle 46).

Site 975

Site 975 is located on the Menorca Rise between the Balearic Promontory (Menorca and Mallorca Islands) and the South Balearic

Table 2. Position of calcareous nannofossil events in Hole 974B, as indicated in Figure 2.

Hole 974B				
Event	Biostratigraphic datum	Core, section, interval (cm)	Depth (mbsf)	Depth (mcd)
1. FO	<i>Emiliana huxleyi</i> > <i>Gephyrocapsa</i> spp.	1H-4, 26; 1H-2, 29	4.76-1.79	4.76-1.79
2. FcO	<i>Emiliana huxleyi</i>	1H-4, 26; 1H-2, 29	4.76-1.79	4.76-1.79
3. FO	<i>Emiliana huxleyi</i>	2H-4, 3; 2H-2, 105	11.03-9.05	12.13-10.15
4. LO	<i>Pseudoemiliana lacunosa</i>	3H-3, 61; 3H-3, 7	19.61-19.07	20.99-20.45
5. LO	<i>Pseudoemiliana lacunosa lacunosa</i> (>7)	3H-4, 39; 3H-3, 76	21.49-19.76	22.87-21.14
6. LO acme	<i>Pseudoemiliana lacunosa</i>	5H-4, 143; 5H-3, 99	40.93-38.99	43.43-41.49
7. LO	<i>Crenalithus asanoi</i> (cir.; >6.5)	5H-5, 118; 5H-4, 143	42.18-40.93	44.68-43.43
8. FO	<i>Gephyrocapsa omega</i> (>4)	6H-5, 110; 6H-5, 37	51.60-50.87	54.94-54.21
9. FO	<i>Crenalithus asanoi</i> (cir.; >6.5)	7H-4, 113; 7H-3, 115	59.34-57.86	63.87-62.39
10. LO	<i>Gephyrocapsa</i> spp. (>6.5)	7H-CC; 7H-7, 29	63.91-62.99	68.44-67.52
11. LcO	<i>Helicosphaera sellii</i>	8H-1, 73; 7-CC	64.23-63.91	69.51-68.44
12. FO acme	<i>Pseudoemiliana lacunosa</i>	8H-4, 26; 8H-4, 16	68.16-68.06	73.44-73.34
13. FO	<i>Gephyrocapsa oceanica</i> (>6.5)	8H-7, 74; 8H-6, 107	73.14-71.97	78.42-77.25
14. FO	<i>Gephyrocapsa caribbeanica</i> (>6.5) and <i>Gephyrocapsa oceanica</i> (>6.3)	8H-CC; 8H-7-74	73.54-73.14	78.82-78.42
15. FO	<i>Gephyrocapsa oceanica</i> (>5.5)	9H-1, 144; 9H-1, 134	74.44-74.34	80.34-80.24
16. FO	<i>Gephyrocapsa</i> spp. (>5)	9H-3, 58; 9H-3, 37	76.48-76.27	82.38-82.17
17. LO	<i>Calcidiscus macintyreii</i> (cir.; >11)	9H-3, 73; 9H-3, 58	76.63-76.48	82.53-82.38
18. FO	<i>Gephyrocapsa oceanica</i> (>4)	9H-6, 25; 9H-6, 7	80.65-80.47	86.55-86.37
19. LO	<i>Discoaster brouweri</i>	11H-3, 18; 11H-2, 104	95.18-94.55	99.08-98.45

Notes: LO = last occurrence, FO = first occurrence, LcO = last consistent occurrence, FcO = first consistent occurrence.

Table 3. Astronomical ages of biostratigraphic datums in Hole 974B, as indicated in Figure 2.

Hole 974B				
Event	Biostratigraphic datum	Age (Ma)	Depth (mcd)	
1. FO	<i>Emiliana huxleyi</i> > <i>Gephyrocapsa</i> spp.	0.071	1.79	
2. FcO	<i>Emiliana huxleyi</i>	0.218	4.76	
3. FO	<i>Emiliana huxleyi</i>	0.274	11.14	
4. LO	<i>Pseudoemiliana lacunosa</i>	0.408	20.72	
5. LO	<i>Pseudoemiliana lacunosa lacunosa</i> (>7)	0.430	22.00	
6. LO acme	<i>Pseudoemiliana lacunosa</i>	0.751	42.46	
7. LO	<i>Crenalithus asanoi</i> (cir.; >6.5)	0.781	44.05	
8. FO	<i>Gephyrocapsa omega</i> (>4)	0.964	54.08	
9. FO	<i>Crenalithus asanoi</i> (cir.; >6.5)	1.122	62.39	
10. LO	<i>Gephyrocapsa</i> spp. (>6.5)	1.243	67.98	
11. LcO	<i>Helicosphaera sellii</i>	1.272	69.35	
12. FO acme	<i>Pseudoemiliana lacunosa</i>	1.359	73.39	
13. FO	<i>Gephyrocapsa oceanica</i> (>6.5)	1.498	77.83	
14. FO	<i>Gephyrocapsa caribbeanica</i> (>6.5) and <i>Gephyrocapsa oceanica</i> (>6.3)	1.521	78.62	
15. FO	<i>Gephyrocapsa oceanica</i> (>5.5)	1.566	80.29	
16. FO	<i>Gephyrocapsa</i> spp. (>5)	1.615	82.27	
17. LO	<i>Calcidiscus macintyreii</i> (cir.; >11)	1.619	82.45	
18. FO	<i>Gephyrocapsa oceanica</i> (>4)	1.721	86.46	
19. LO	<i>Discoaster brouweri</i>	1.954	98.76	

Notes: LO = last occurrence, FO = first occurrence, LcO = last consistent occurrence, FcO = first consistent occurrence.

Basin (Fig. 1). Four holes were drilled at about 2415 m water depth and a complete Pleistocene sequence was cored. Thirty-six sapropels (coded 501 to 536) correlated to thirty-two insolation cycles, were recorded with TOC MAX contents ranging from 0.8% to 2.9% (Comas, Zahn, Klaus, et al., 1996; Murat, Chap. 41, this volume). Some insolation cycles are composite, composed of two or three, thin sapropels (e.g., i-cycles 18, 58, and 90). Depths, coding, and characteristics of the sapropels are given by Murat (Chap. 41, this volume). Calcareous nannofossils are very abundant and many intervals contain coccolith oozes. Sampling spacing is on average three samples per section with a 10-cm sampling interval in sapropel sequences. A precise biostratigraphic framework based on 20 datums was used to correlate the sapropels with the insolation cycle (Fig. 3) and to date the magnetic reversal boundaries. Compared to the biostratigraphy established on board and based on seven Pleistocene datums (Comas, Zahn, Klaus, et al., 1996), this new Pleistocene biostratigraphic framework allows a more precise correlation and better estimation of the sedimentation rates. It also provides some fixpoints to calibrate the oxygen isotopic events and to construct the initial age model at Site 975 (Pierre et al.,

Chap. 38, this volume). The nannofossil events used to date the Pleistocene interval are listed in Tables 4 (depth) and 5 (estimated ages). Figure 3 presents the correlation of the sapropels recognized at Site 975 with the insolation cycles (astronomical precession cycles with a time lag of 3 k.y.).

The LO of *Discoaster brouweri* occurs at BID of 146.56 mcd in Hole 975B (Tables 4, 5). The age of this datum is estimated at 1.95 Ma by Lourens et al. (1996a) and lies in i-cycle 189 (1.954 Ma). The base of the Olduvai Chron, dated at 1.942 Ma by Lourens et al. (1996a), is inferred at Site 975 at 144.79 mcd, based on a position in Hole 975B at 137.0 mbsf, and occurs in i-cycle 188. The top of the Olduvai Chron is placed at 121.5 mbsf in Hole 975C, which corresponds to 120.26 mbsf (129.30 mcd) in Hole 975B. The age of this boundary is estimated at 1.786 Ma by Lourens et al. (1996a) and occurs in i-cycle 174.

The oldest small-scale cluster of sapropels 536 to 534 corresponds to the sapropel cluster pattern “e–h” in Vrica. The Pliocene/Pleistocene boundary (1.806 Ma) is situated at the top of the “e” sapropel (i-cycle 176), which corresponds to the top of sapropel 536 at 131.28 mcd (Fig. 3). Sapropel 535 corresponds to the “f” sapropel in Vrica (i-cycle 170 at 1.736 Ma). Sapropel 534 corresponds to the “h” sapropel in Vrica (i-cycle 168 at 1.715 Ma) and is situated at 126.11 mcd. In Hole 975C, the FO of *Gephyrocapsa caribbeanica* is situated at BID of 126.33 mcd and the FO of *Gephyrocapsa oceanica* (>4) is observed at BID of 126.20 mcd. In Hole 975B, the FO of *Gephyrocapsa oceanica* (>4) occurs between two cores (Table 4).

From i-cycle 168 (1.715 Ma) to i-cycle 116 (1.222 Ma), only four sapropels were observed (i-cycles 148, 136, 134, and 128). Sapropel 533 (i-cycle 148 at 1.524 Ma) at 113.06 mcd is between datum 14 (FO of *G. caribbeanica* (>6.5 μm) - *G. oceanica* [>6.3 μm]) at 113.15 mcd and datum 13 (FO of *Gephyrocapsa oceanica* [>6.5 μm]) at 112.22 mcd (Fig. 3). Above sapropel 530, two clusters of sapropels are recorded, one from i-cycle 116 (1.222 Ma) to i-cycle 112 (1.185 Ma) and a second from i-cycle 104 (1.111 Ma) to i-cycle 86 (0.908 Ma). Datum 9 (FO *Crenalithus asanoi*) is between i-cycle 112 (1.185 Ma) at 90.665 mcd and i-cycle 104 (1.111 Ma) at 85.64. Datum 8 (FO *Gephyrocapsa omega* [>4]) occurs in the second cluster between i-cycle 90 (0.957 Ma) at 77.10 mcd and i-cycle 86 (0.911 Ma) at 73.25 mcd. Sapropel 518 at 61.53 mcd in Hole 975B corresponds to i-cycle 68 (0.732 Ma) and is situated just above the B/M boundary. Magnetostratigraphic measurements indicate that the B/M boundary (0.78 Ma) is at 64.35 mcd. From i-cycle 60 (0.647 Ma) to i-cycle 12 (0.124 Ma), the sapropel distribution is very similar to the pattern observed at Sites 977 and 979: (1) a cluster of five sapropels composed of i-

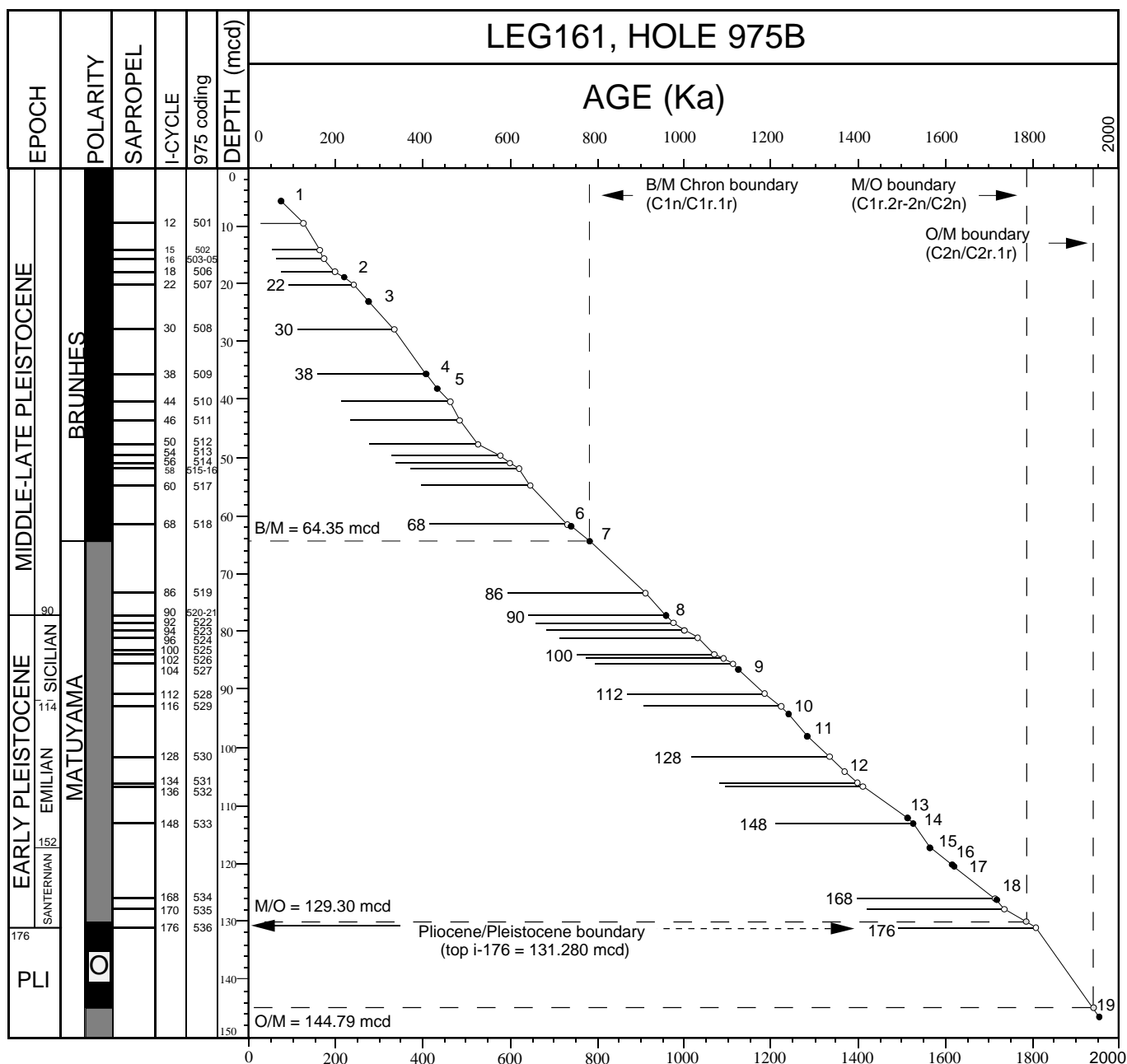


Figure 3. Age-depth plot. Calibration of sapropels in Hole 975B with the insolation cycles. Position and age of calcareous nannofossil events (19 black dots) are from Tables 4 and 5. Sapropels (32 white dots) are numbered (Site 975 coding described by Murat, Chap. 41, this volume) and correlated to the insolation cycle (i-cycle). Ages of i-cycles are indicated in Table 1.

cycles 60 to 50; and (2) presence of sapropels, which pattern corresponds to the sequence of “S” sapropels described for the eastern Mediterranean (Cita et al., 1977). In this succession, only S8 (i-cycle 20 at 0.217 Ma) is not recorded. Uppermost Pleistocene sapropels “S1 to S4” were not observed at Site 975. Datum 4 (LO of *Pseudoemiliania lacunosa*) is at BID of 35.55 mcd and is placed just below the sapropel 509 (i-cycle 38 at 0.405 Ma) at 35.47 mcd. Datum 3 (FO of *Emiliania huxleyi*) is at BID of 23.17 mcd and is situated between i-cycle 22 (“S9”) and i-cycle 30 (“S10”).

Site 976

This site is located in the Western Alboran Sea, 60 km off the southern Spanish coast and 11 km east of the Strait of Gibraltar (Fig.

1). It is about 8 km northeast of Deep Sea Drilling Project (DSDP) Site 121 (Leg 13) in a water depth of 1108 m. Pleistocene sediments were recovered in four holes (976A to 976D). In Holes 976B and 976C, a near-complete, very thick Pleistocene sequence was cored (Cores 161-976B-1H to 40X and Cores 976C-1H to 40X). In Hole 976B, core recovery in the Pleistocene interval was high (100%), except in Cores 976B-3X (35%), 16X (76%), and 21X (30%), and two Cores, 976B-27X and 31X, were lost. Data from Hole 976C filled part of the lost Pleistocene sequence and completed a composite section (mcd [meters composite depth] in Table 4). But the same two intervals also were not recovered in Hole 976C; Cores 21X and 30X were lost. Based on both holes, twenty-nine sapropels (coded 601 to 628, and A27) were recorded with TOC MAX contents ranging from 0.8% to 1.85% (Comas, Zahn, Klaus, et al., 1996; Murat, Chap. 41,

Table 4. Position of calcareous nannofossil events in Hole 975B, as indicated in Figure 3.

Hole 975B					
Event	Biostratigraphic datum	Core, section, interval (cm)	Depth (mbsf)	Depth (mcd)	
1. FO	<i>Emiliana huxleyi</i> > <i>Gephyrocapsa</i> spp.	975B 2H-1, 130; 1H-CC	5.40-4.16	7.13-4.16	
2. FcO	<i>Emiliana huxleyi</i>	975B 3H-4, 15; 3H-2, 136	18.25-16.46	19.75-17.96	
3. FO	<i>Emiliana huxleyi</i>	975B 3H-6, 140; 3H-5, 125	22.50-20.85	24.00-22.35	
4. LO	<i>Pseudoemiliana lacunosa</i>	975B 4H-CC; 4H-CC, 12	32.75-32.65	35.60-35.50	
5. LO	<i>Pseudoemiliana lacunosa lacunosa</i> (>7)	975B 5H-2, 114; 5H-1, 111	35.24-33.71	38.99-37.46	
6. LO acme	<i>Pseudoemiliana lacunosa</i>	975B 7H-4, 127; 7H-4, 93	57.37-57.03	62.12-61.78	
7. LO	<i>Crenalithus asanoi</i> (cir.; >6.5)	975B 7H-CC; 975C-7H-CC	59.97-59.86	64.72-64.23	
8. FO	<i>Gephyrocapsa omega</i> (>4)	975B 8H-CC; 8H-7, 43	70.91-70.44	77.31-76.84	
9. FO	<i>Crenalithus asanoi</i> (cir.; >6.5)	975B 9H-CC; 9H-6, 146	80.56-79.56	86.87-85.87	
10. LO	<i>Gephyrocapsa</i> spp. (>6.5)	975B 10H-6, 120; 10H-4, 143	88.80-86.03	95.60-92.83	
11. LcO	<i>Helicosphaera sellii</i>	975B 11H-2, 111; 11H-1, 109	92.21-90.69	98.76-97.24	
12. FO acme	<i>Pseudoemiliana lacunosa</i>	975B 11H-6, 112; 11H-5, 112	98.22-96.72	104.77-103.27	
13. FO	<i>Gephyrocapsa oceanica</i> (>6.5)	975B 12H-5, 90-92; 12H-4, 111	106.00-104.71	112.87-111.58	
14. FO	<i>Gephyrocapsa caribbeanica</i> (>6.5) and <i>Gephyrocapsa oceanica</i> (>6.3)	975B 12H-5, 121; 12H-5, 116	106.31-106.26	113.18-113.13	
15. FO	<i>Gephyrocapsa oceanica</i> (>5.5)	975B 13H-1, 107; 13H-1, 100	109.67-109.60	117.37-117.30	
		975C 13H-3, 43; 13H-3, 30	110.33-110.20	(117.30-117.17)	
		975 975		(adopted depth 117.30)	
16. FO	<i>Gephyrocapsa</i> spp. (>5)	975B 13H-4, 110; 13H-3, 90	112.67-112.50	120.37-120.20	
		975C 13H-5, 50; 13H-4, 30	113.40-113.20	(120.37-120.17)	
		975 975		(adopted depth 120.20)	
17. LO	<i>Calcidiscus macintyreii</i> (cir.; >11)	975B 13H-4, 110; 13H-3, 90	112.67-112.50	120.37-120.20	
		975C 13H-5, 50; 13H-4, 30	113.40-113.20	(120.37-120.17)	
		975 975		(adopted depth 120.37)	
18. FO	<i>Gephyrocapsa oceanica</i> (>4)	975B 14H-1, 123; 13H-CC	119.33-118.66	128.37-126.36	
		975C 14H-3, 50; 14H-3, 30	118.50-118.30	(126.30-126.10)	
FO	<i>Gephyrocapsa caribbeanica</i> (>4)	975C 14H-3, 57; 14H-3, 50	118.57-118.50	(126.37-126.30)	
FO	<i>Gephyrocapsa</i> s.l. (>4)	975 975		(adopted depth 126.33)	
19. LO	<i>Discoaster brouweri</i>	975B 16H-1, 131; 15H-CC	138.41-137.82	146.32-146.8	

Notes: Hole 975C was used to position Events 15–18 more precisely in the composite depth section. LO = last occurrence, FO = first occurrence, LcO = last consistent occurrence, FcO = first consistent occurrence.

Table 5. Astronomical ages of biostratigraphic datums in Hole 975B, as indicated in Figure 3.

Hole 975B				
Event	Biostratigraphic datum	Age (Ma)	Depth (mcd)	
1. FO	<i>Emiliana huxleyi</i> > <i>Gephyrocapsa</i> spp.	0.071	5.64	
2. FcO	<i>Emiliana huxleyi</i>	0.219	18.85	
3. FO	<i>Emiliana huxleyi</i>	0.274	23.17	
4. LO	<i>Pseudoemiliana lacunosa</i>	0.406	35.55	
5. LO	<i>Pseudoemiliana lacunosa lacunosa</i> (>7)	0.432	38.22	
6. LO acme	<i>Pseudoemiliana lacunosa</i>	0.739	61.95	
7. LO	<i>Crenalithus asanoi</i> (cir.; >6.5)	0.781	64.48	
8. FO	<i>Gephyrocapsa omega</i> (>4)	0.956	77.07	
9. FO	<i>Crenalithus asanoi</i> (cir.; >6.5)	1.122	86.37	
10. LO	<i>Gephyrocapsa</i> spp. (>6.5)	1.237	94.21	
11. LcO	<i>Helicosphaera sellii</i>	1.284	98.00	
12. FO acme	<i>Pseudoemiliana lacunosa</i>	1.369	104.02	
13. FO	<i>Gephyrocapsa oceanica</i> (>6.5)	1.498	112.22	
14. FO	<i>Gephyrocapsa caribbeanica</i> (>6.5) and <i>Gephyrocapsa oceanica</i> (>6.3)	1.513	113.15	
15. FO	<i>Gephyrocapsa oceanica</i> (>5.5)	1.525	117.30	
16. FO	<i>Gephyrocapsa</i> spp. (>5)	1.616	120.20	
17. LO	<i>Calcidiscus macintyreii</i> (cir.; >11)	1.619	120.28	
18. FO	<i>Gephyrocapsa oceanica</i> (>4)	1.718	126.33	
19. LO	<i>Discoaster brouweri</i>	1.954	146.56	

Notes: LO = last occurrence, FO = first occurrence, LcO = last consistent occurrence, FcO = first consistent occurrence.

this volume). Sampling interval is on average, two samples per section with a 15-cm sampling interval in sapropel sequences. Calcareous nannofossils are very abundant at this site. A precise biostratigraphic framework based on 16 datums (Tables 6 and 7) provides the time scale to date the sapropels and to calibrate the oxygen isotope stratigraphy (von Grafenstein et al., Chap. 37, this volume). No magnetostratigraphic zones were recognized at Site 976 because of demagnetization of the cores. Magnetostratigraphic chron boundaries in Figure 4 are given for comparison with data obtained at Sites 974 and 975 and to approximate a possible depth for these boundaries on the age-depth plot. The nannofossil events used to date the Pleistocene interval are listed in Tables 6 (depth) and 7 (estimated ages). Figure 4 presents the calibration of the sapropels recognized at Site 976 with the insolation cycles (astronomical precession cycles with a

time lag of 3 k.y.). One insolation cycle (i-cycle 90) is composed of two sapropels (621 and 622).

The absence of sapropels at this site below i-cycle 148 (1.524 Ma) prevents the identification of the Pliocene/Pleistocene boundary. By extrapolating the age-depth plot to 1.806 Ma, the Pliocene/Pleistocene boundary may be estimated at about 373 mcd. Datum 14 (FO of *G. caribbeanica* [>6.5 μm]-*G. oceanica* [>6.3 μm]) occurs between 323.35 and 322.50 mcd (BID 322.92 mcd), and is just above the sapropel 628 (i-cycle 148 at 1.524 Ma) at 327.01 mcd. A first small-scale cluster of three sapropels (A27, 627, and 626) is placed by datum 12 (FO acme of *Pseudoemiliana lacunosa*) at BID of 299.51 mcd and corresponds to the “*-u” cluster in Vrica. Datum 12 occurs in i-cycle 130 (1.356 Ma). Precise depths for datums 11 and 10 could not be determined (depths are in parentheses in Table 6) and the two datums are not used in the age-depth plot. Both datums occur in one of the lost cores of Site 976.

A second small-scale cluster of three sapropels (i-cycle 108 to 98) occurs near datum 9 (FO of *Crenalithus asanoi*). This datum is placed at BID of 266.57 mcd and is between sapropel 625 (i-cycle 108 at 1.144 Ma) at 269.74 mcd and sapropel 624 (i-cycle 104 at 1.111 Ma) at 264.91 mcd. Sapropels 621 (241.94 mcd) and 622 (241.905 mcd) are correlated to the same high-amplitude maximum of i-cycle 90 (at 0.955 Ma). Datum 8 (FO *Gephyrocapsa omega* [>4 μm]) occurs shortly before i-cycle 90. This datum is at BID of 244.31 mcd. A third small-scale cluster of four sapropels (619–616) correlates to i-cycles 68, 67, 66, and 64. Sapropel 616 corresponds to high-amplitude insolation maximum of i-cycle 64 at 0.690 Ma. Datum 6 (LO acme of *Pseudoemiliana lacunosa*) is at BID of 194.48 mcd, shortly before i-cycle 68 (at 0.732 Ma) at 190.30 mcd.

In the upper Pleistocene, the typical “S” sapropel sequence described from the eastern Mediterranean (Cita et al., 1977) is recorded and includes i-cycles 30 (“S10”), 22 (“S9”), 20 (“S8”), 18 (“S7”), 16 (“S6”), 12 (“S5”), 10 (“S4”), 8 (“S3”), and 6 (“S2”). From this sequence, the “S12,” which corresponds to i-cycle 46 (0.483 Ma) and the “S11,” which corresponds to i-cycle 38 (0.407 Ma), were not observed. Oxygen isotope stratigraphy indicates that Sapropels 613 and 612 correspond respectively to i-cycle 48 (at 0.503 Ma) and to i-cycle 40 (at 0.425 Ma). Sapropel 601 is between 4.95 mcd and 3.64 mcd (BID at 4.295 mcd). Calibration of sapropel 601 to the oxygen iso-

Table 6. Position of calcareous nannofossil events in Hole 976B, as indicated in Figure 4.

Hole 976B		Core, section, interval (cm)	Depth (mbsf)	Depth (mcd)
Event	Biostratigraphic datum			
1. FO	<i>Emiliania huxleyi</i> > <i>Gephyrocapsa</i> spp	4H-4, 100; 4H-3, 100	28.00-26.50	28.18-26.68
2. FcO	<i>Emiliania huxleyi</i>	7H-6, 103; 7H-5, 103	59.53-58.03	59.71-58.21
3. FO	<i>Emiliania huxleyi</i>	9H-4, 119; 9H-4, 100	75.59-75.50	76.60-76.51
4. LO	<i>Pseudoemiliania lacunosa</i>	13H-4, 74; 13H-3, 100	112.24/111.98	116.24-115.98
5. LO	<i>Pseudoemiliania lacunosa lacunosa</i> (>7)	13H-6, 100; 13H-5, 100	116.50-115.00	120.50-119.00
6. LO acme	<i>Pseudoemiliania lacunosa</i>	22X-1, 100; 21X-CC	195.40-187.62	198.37-190.59
7. LO	<i>Crenalithus asanoi</i> (cir.; >6.5)	22X-5, 100; 22X-4, 100	201.40-199.90	204.37-202.87
8. FO	<i>Gephyrocapsa omega</i> (>4)	26X-CC; 26X-7, 99	242.15-241.04	244.87-243.76
9. FO	<i>Crenalithus asanoi</i> (cir.; >6.5)	29X-3, 100; 29X-2, 100	264.60-263.10	267.32-265.82
10. LO	<i>Gephyrocapsa</i> spp. (>6.5)	32X-1, 4; 30X-CC	[294.03-281.39]	[293.28-284.64]
11. LcO	<i>Helicosphaera sellii</i>	32X-1, 4; 30X-CC	[294.03-281.39]	[293.28-284.64]
12. FO acme	<i>Pseudoemiliania lacunosa</i>	32X-CC; 32X-7, 100	299.87-299.34	(299.16-298.59)
13. FO	<i>Gephyrocapsa oceanica</i> (>6.5)	34X-5, 99; 34X-4, 100	316.43-314.94	319.12-317.63
14. FO	<i>Gephyrocapsa caribbeanica</i> (>6.5) and <i>Gephyrocapsa oceanica</i> (>6.3)	35X-2, 100; 34X-CC	321.48-319.81	323.35-322.50
15. FO	<i>Gephyrocapsa oceanica</i> (>5.5)	36X-CC; 36X-7, 100	338.67-337.78	(340.25-339.36)
16. FO	<i>Gephyrocapsa</i> spp. (>5)	37X-7, 98; 37X-6, 100	347.75-346.36	349.33-347.94
17. LO	<i>Calcidiscus macintyreii</i> (cir., >11)	38X-2, 83; 37X-CC	350.43-348.21	350.43-348.21
18. FO	<i>Gephyrocapsa oceanica</i> (>4)	39X-1, 100; 38X-CC	358.71-357.92	364.18-357.92

Notes: LO = last occurrence, LcO = last consistent occurrence, FO = first occurrence, FcO = first consistent occurrence. Depths in parentheses indicate that samples do not belong to the composite section. Depths in square brackets indicate that datums occur within a lost core interval.

Table 7. Astronomical ages of biostratigraphic datums in Hole 976B, as indicated in Figure 4.

Hole 976B		Age (Ma)	Depth (mcd)
Event	Biostratigraphic datum		
1. FO	<i>Emiliania huxleyi</i> > <i>Gephyrocapsa</i> spp.	0.072	27.53
2. FcO	<i>Emiliania huxleyi</i>	0.218	58.96
3. FO	<i>Emiliania huxleyi</i>	0.270	76.55
4. LO	<i>Pseudoemiliania lacunosa</i>	0.424	116.11
5. LO	<i>Pseudoemiliania lacunosa lacunosa</i> (>7)	0.439	119.75
6. LO acme	<i>Pseudoemiliania lacunosa</i>	0.746	194.48
7. LO	<i>Crenalithus asanoi</i> (cir.; >6.5)	0.778	203.62
8. FO	<i>Gephyrocapsa omega</i> (>4)	0.962	244.31
9. FO	<i>Crenalithus asanoi</i> (cir.; >6.5)	1.122	266.57
10. LO	<i>Gephyrocapsa</i> spp. (>6.5)	N/A	N/A
11. LcO	<i>Helicosphaera sellii</i>	N/A	N/A
12. FO acme	<i>Pseudoemiliania lacunosa</i>	1.358	299.51
13. FO	<i>Gephyrocapsa oceanica</i> (>6.5)	1.493	318.37
14. FO	<i>Gephyrocapsa caribbeanica</i> (>6.5) and <i>Gephyrocapsa oceanica</i> (>6.3)	1.516	322.92
15. FO	<i>Gephyrocapsa oceanica</i> (>5.5)	1.569	339.98
16. FO	<i>Gephyrocapsa</i> spp. (>5)	1.613	348.63
17. LO	<i>Calcidiscus macintyreii</i> (cir., >11)	1.619	349.32
18. FO	<i>Gephyrocapsa oceanica</i> (>4)	1.718	361.05

Note: LO = last occurrence, FO = first occurrence, LcO = last consistent occurrence, FcO = first consistent occurrence.

tope records assigns an age between 14.51 Ka and 10.31 Ka (best interpolated age of 12.41 Ka). In the eastern Mediterranean, the "S1" is correlated to i-cycle 2 at 8 Ka (Hilgen, 1991; Lourens et al., 1996a). Sapropel 601 is older than "S1." The age of sapropel 601 corresponds to the Younger Dryas (Y.D.) oxygen isotope event calibrated at 11.5 Ka (von Grafenstein et al., Chap. 37, this volume).

Site 977

This site is located south of Cabo de Gata in the Eastern Alboran Basin, halfway between the Algerian and the Spanish coasts (Fig. 1). One hole was drilled in a water depth of 1985 m. A very thick Pleistocene sequence was cored and fifty sapropels, coded 701 to 750 (Fig. 5) were recorded with TOC MAX contents ranging from 0.7% to 2.1% (Comas, Zahn, Klaus, et al., 1996; Murat, Chap. 41, this volume). Calcareous nannofossils are very abundant and three intervals contain *Braarudosphaera bigelowii* (Br.) oozes (Fig. 5). The bio-

stratigraphic framework is similar to that developed at Sites 974 and 975. The same eighteen datums are used to correlate the fifty sapropels to insolation cycles, to calibrate the oxygen isotope records, and to correlate results from Site 977 with the other Leg 161 sites. No magnetostratigraphic data were obtained at Site 977 because of demagnetization and overprinting, as observed also at Site 976. Magnetostratigraphic chron boundaries in Figure 5 are given to approximate a possible depth for these boundaries on the age-depth plot and for comparison with the other sites. The nannofossil events used to date this interval are listed in Tables 8 (depth) and 9 (estimated ages). Figure 5 presents an age-depth plot, the stratigraphic position of the calcareous nannofossil events relative to the sapropels, and the correlation of Site 977 sapropels with the insolation cycle codification (astronomical precession cycles with a time lag of 3 ka). Some insolation cycles are composed of two (i-cycles 12, 22, 30, 64, 94, and 98), or three (i-cycle 10) sapropels.

The absence of lowermost Pleistocene sapropels below i-cycle 144 (1.490 Ma) does not allow a precise determination of the Pliocene/Pleistocene boundary. By extrapolating the age-depth plot to 1.806 Ma, the Pliocene/Pleistocene is at about 276 mbsf. The age-depth plot (Fig. 5) indicates that very little change in accumulation rate occurred in the Pleistocene and that sapropel distribution is arranged in small-scale clusters. A first small-scale cluster of sapropels is observed between sapropels 748 and 744. This cluster is centered on the high-amplitude insolation maxima of i-cycle 130 (1.356 Ma), which is correlated to the thick sapropel 747. Datum 12 (FO acme of *Pseudoemiliania lacunosa*) is at BID of 211.31 mbsf and just below sapropel 747. Datum 11 (LcO of *Helicosphaera sellii*) is at BID of 202.24 mbsf and just above sapropel 744 (i-cycle 122 at 1.280 Ma). The next sapropel above this cluster, sapropel 743 (i-cycle 112 at 1.185 Ma) at 194.17 mbsf, is just above datum 10 (LO *Gephyrocapsa* spp. [>6.5 μm]) at BID of 195.71 mbsf. Based on oxygen isotope stratigraphy, a gap exists between Core 25X and Core 24X (von Grafenstein et al., Chap. 37, this volume). A second small-scale cluster of sapropels (sapropels 743 to 741) is centered on the high-amplitude insolation maximum of i-cycle 110 (at 1.164 Ma) and contain i-cycles 112 to 108. A third small-scale cluster of sapropels (740 to 737) is placed by the high-amplitude insolation maximum of i-cycle 100 (at 1.070 Ma), which is correlated to sapropel 740 at 177.24 mbsf. A fourth small-scale cluster of sapropels (736 to 732) is placed by datum 8 (FO *Gephyrocapsa omega* [>4 μm]). This datum is at BID

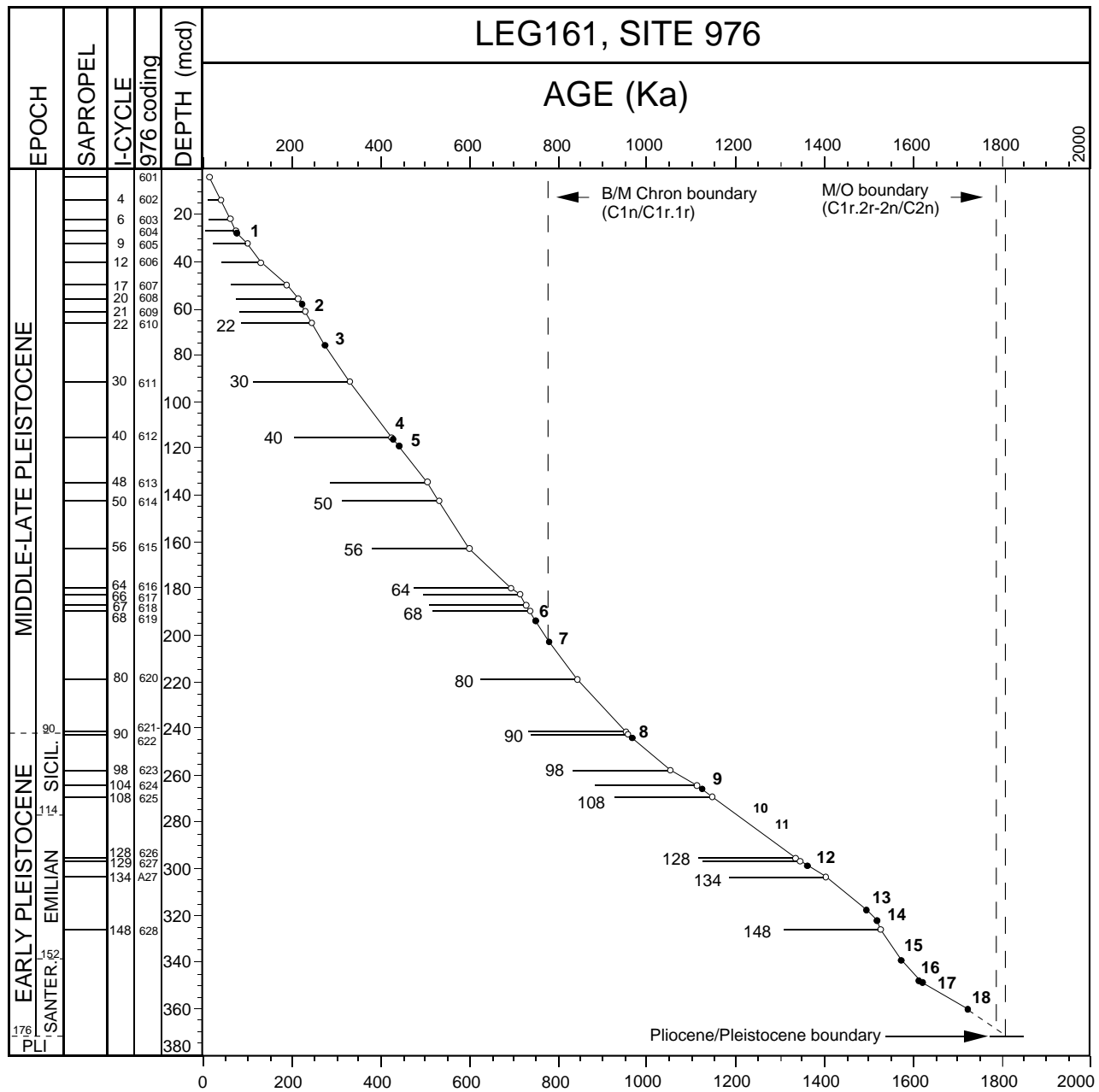


Figure 4. Age-depth plot. Calibration of sapropels at Site 976 with the insolation cycles. Position and age of calcareous nannofossil events (18 black dots) are from Tables 6 and 7. Sapropels (28 white dots) are numbered (Site 976 coding described by Murat, Chap. 41, this volume) and correlated to the insolation cycle (i-cycle). Ages of i-cycles are indicated in Table 1.

of 158.55 mbsf and between sapropels 734 and 733. Sapropel 733 (at 156.22 mbsf) is correlated to the high-amplitude insolation maximum of i-cycle 90 (at 0.955 Ma).

In middle-late Pleistocene sediments at Site 977, three small-scale clusters of sapropels are distinct and clearly reflected in the La90_(1,1) summer insolation curve:

1. A first cluster of six sapropels (730–725) correlates to i-cycles 72 to 62. Sapropels 726 and 727 are correlated to the high-amplitude insolation maximum of i-cycle 64 at 0.690 Ma;
2. A second cluster of three sapropels (724–722) correlates to i-cycles 58 to 54; and

3. A third cluster of four sapropels (721–718) correlates to i-cycles 52 to 48.

Datum 7 (*LO Crenalithus asanoi* [$>6.5 \mu\text{m}$]) is placed at BID of 125.30 mbsf, just below the sapropel 730 (i-cycle 72 at 0.765 Ma). Datum 6 (LO acme of *Pseudoemiliania lacunosa*) is at BID of 120.29 mbsf and between sapropel 730 (i-cycle 72 at 123.73 mbsf) and sapropel 729 (i-cycle 68 at 118.58 mbsf).

Uppermost Pleistocene sapropel succession is well correlated to the sequence of “S” sapropels described by Cita et al. (1977) in the eastern Mediterranean. It includes “S10” (715–714), “S9” (712–711), “S7” (710), “S6” (709), “S5” (708–707), “S4” (706–704), and

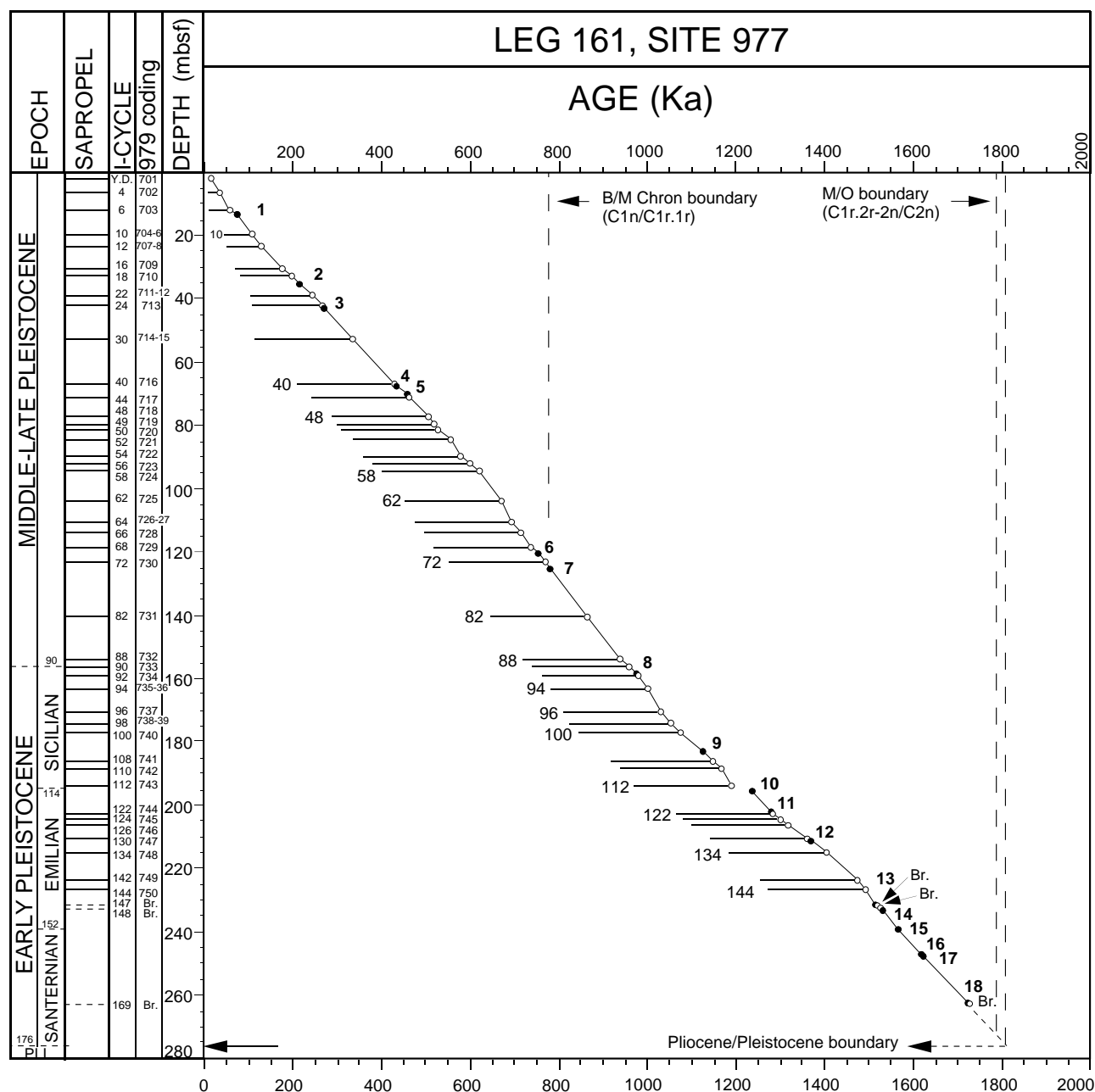


Figure 5. Age-depth plot. Calibration of sapropels at Site 977 with the insolation cycles. Position and age of calcareous nannofossil events (18 black dots) are from Tables 8 and 9. Sapropels (42 white dots) are numbered (Site 977 coding described by Murat, Chap. 41, this volume) and correlated to the insolation cycle (i-cycle). Ages of i-cycles are indicated in Table 1. Br. = *Braarudosphaera bigelowii* bloom.

“S3” (703). Datum 4 (LO *Pseudoemiliana lacunosa*) is situated at BID of 68.07 mbsf and just below sapropel 716 (i-cycle 40) at 67.18 mbsf. Datum 2 (FcO *Emiliana huxleyi*) is situated at BID of 35.48 mbsf and between i-cycle 22 (0.240 Ma) at 39.23 mbsf and i-cycle 18 (0.195 Ma) at 33.0 mbsf. The i-cycle 22 contains two sapropels (double), 711 at 38.99 mbsf and 712 at 39.47 mbsf. Sapropel 702 is correlated with the i-cycle 4 (0.035 Ma) and sapropel 701 to the Y. Dryas (Y.D.) oxygen isotope event calibrated at 11.50 Ka (von Grafenstein et al., Chap. 37, this volume).

Site 979

Site 979 is located in the southern Alboran Basin, a narrow depression between Alboran Island and the Moroccan coast at 45 km

away. Site 979 is at 1062 m water depth and consists of one hole with a complete and thick Pleistocene sequence. The sediments recovered were uniform and consisted mainly of hemipelagic deposits with abundant and well-preserved calcareous nannofossils throughout the section, except for the bottom of the sapropels, where we observed variable nannofossil abundances and dissolution. Forty-eight Pleistocene sapropels were observed with TOC MAX contents ranging from 0.8% to 2.2% (Comas, Zahn, Klaus, et al., 1996; Murat, Chap. 41, this volume). A succession of 22 datums was used for the biostratigraphic framework at Site 979, which provides the calibration to date the sapropels. No magnetostratigraphy events were identified because of overprinting throughout the cores, and no oxygen isotope analyses are yet available for this site. The average sampling interval for nannofossil analysis at Site 979 is two samples per section with

Table 8. Astronomical ages of biostratigraphic datums in Hole 977A, as indicated in Figure 5.

Hole 977A			
Event	Biostratigraphic datum	Core, section, interval (cm)	Depth (mbsf)
1. FO	<i>Emiliana huxleyi</i> > <i>Gephyrocapsa</i> spp.	2H-CC, 11-12; 2H-7, 40-41	13.77-13.33
2. FcO	<i>Emiliana huxleyi</i>	5H-2, 125-126; 5H-2, 91-92	35.70-35.25
3. FO	<i>Emiliana huxleyi</i>	6H-2, 20-21; 6H-1, 140-141	43.70-43.40
4. LO	<i>Pseudoemiliana lacunosa</i>	8H-5, 140-141; 8H-5, 74-76	68.40-67.74
5. LO	<i>Pseudoemiliana lacunosa lacunosa</i> (>7)	8H-7, 40-41; 8H-7, 20-21	70.40-70.20
6. LO acme	<i>Pseudoemiliana lacunosa</i>	14H-2, 90-91; 14H-2, 72-74	120.40-120.22
7. LO	<i>Crenalithus asanoi</i> (cir.; >6.5)	14H-5, 140-141; 14H-5, 120-121	125.40-125.20
8. FO	<i>Gephyrocapsa omega</i> (>4)	18X-2, 120-121; 18X-2, 90-91	158.70-158.40
9. FO	<i>Crenalithus asanoi</i> (cir.; >6.5)	20X-6, 83-84; 20X-5, 142-143	183.53-182.62
10. LO	<i>Gephyrocapsa</i> spp. (>6.5)	22X-1, 142; 22X-1, 120-121	195.82-195.60
11. LcO	<i>Helicosphaera sellii</i>	22X-6, 43-44; 22X-6, 25-26	202.33-202.15
12. FO acme	<i>Pseudoemiliana lacunosa</i>	23X-5, 141-142; 23X-5, 120-121	211.41-211.21
13. FO	<i>Gephyrocapsa oceanica</i> (>6.5)	25X-6, 86-87; 25X-6, 64-65	231.59-231.37
14. FO	<i>Gephyrocapsa caribbeanica</i> (>6.5) and <i>Gephyrocapsa oceanica</i> (>6.3)	26X-1, 69-70; 26X-1, 41-42	233.69-233.41
15. FO	<i>Gephyrocapsa oceanica</i> (>5.5)	26X-5, 120-121; 26X-5, 62-63	240.10-239.52
16. FO	<i>Gephyrocapsa</i> spp. (>5)	27X-4, 94-95; 27X-3, 137-138	248.04-246.97
17. LO	<i>Calcidiscus macintyreii</i> (cir., >11)	27X-4, 121-122; 27X-4, 94-95	248.31-248.04
18. FO	<i>Gephyrocapsa oceanica</i> (>4)	29X-1, 120-121; 29X-1, 65-66	263.00-262.45

Note: LO = last occurrence, FO = first occurrence, LcO = last consistent occurrence, FcO = first consistent occurrence.

Table 9. Astronomical ages of biostratigraphic datums in Hole 977A, as indicated in Figure 5.

Hole 977A			
Event	Biostratigraphic datum	Age (Ma)	Depth (mbsf)
FO	<i>Emiliana huxleyi</i> > <i>Gephyrocapsa</i> spp.	0.070	13.55
2. FcO	<i>Emiliana huxleyi</i>	0.213	35.48
3. FO	<i>Emiliana huxleyi</i>	0.269	43.55
4. LO	<i>Pseudoemiliana lacunosa</i>	0.429	68.07
5. LO	<i>Pseudoemiliana lacunosa lacunosa</i> (>7)	0.454	70.30
6. LO acme	<i>Pseudoemiliana lacunosa</i>	0.752	120.29
7. LO	<i>Crenalithus asanoi</i> (cir.; >6.5)	0.777	125.30
8. FO	<i>Gephyrocapsa omega</i> (>4)	0.973	158.55
9. FO	<i>Crenalithus asanoi</i> (cir.; >6.5)	1.122	183.08
10. LO	<i>Gephyrocapsa</i> spp. (>6.5)	1.235	195.71
11. LcO	<i>Helicosphaera sellii</i>	1.276	202.24
12. FO acme	<i>Pseudoemiliana lacunosa</i>	1.361	211.31
13. FO	<i>Gephyrocapsa oceanica</i> (>6.5)	1.512	231.48
14. FO	<i>Gephyrocapsa caribbeanica</i> (>6.5) and <i>Gephyrocapsa oceanica</i> (>6.3)	1.529	233.55
15. FO	<i>Gephyrocapsa oceanica</i> (>5.5)	1.563	239.81
16. FO	<i>Gephyrocapsa</i> spp. (>5)	1.614	247.51
17. LO	<i>Calcidiscus macintyreii</i> (cir., >11)	1.619	248.17
18. FO	<i>Gephyrocapsa oceanica</i> (>4)	1.719	262.73

Note: LO = last occurrence, FO = first occurrence, LcO = last consistent occurrence, FcO = first consistent occurrence.

higher resolution of about one sample per 15 cm in the sapropel sequences. The nannofossil biostratigraphic events used to date the Pleistocene interval are listed in Tables 10 (depth) and 11 (estimated ages). Figure 6 presents an age-depth plot, the stratigraphic position of the calcareous nannofossil events relative to the sapropels, and the correlation of the Site 979 sapropels with the insolation cycle codification (astronomical precession cycles with a time lag of 3 k.y.). Composite (double) sapropels are present in i-cycles 20, 38, 58, 64, and 72, and triple sapropels occur in i-cycle 22.

The Pliocene/Pleistocene boundary (1.806 Ma) is at 356.08 mbsf at the top of sapropel 948, which corresponds to i-cycle 176 at 1.808 Ma. From the twenty Pliocene sapropels recognized between Cores 161-979A-39X and 61X (949 to 968), only sapropels 949 to 952 are calibrated and indicated in Figure 6. Sapropel 952 is correlated with the i-cycle 208 (2.137 Ma). The LOs of *Discoaster brouweri* and *Discoaster triradiatus* occur between samples 979A-43X-CC (at 398.09 mbsf) and -44X-1, 120-121 cm (at 399.30 mbsf). The age of this biohorizon is estimated at 1.95 Ma by Lourens et al. (1996a) and is situated in i-cycle 189 (1.954 Ma). Sapropel 951 at 397.07 mbsf is observed just above the LO of *Discoaster brouweri* (BID at 398.67 mbsf) and is calibrated to i-cycle 188 at 1.944 Ma.

In the lower Pleistocene interval, twelve sapropels were described between i-cycles 168 (1.715 Ma) and 100 (1.070 Ma). Datum 13 (FO *Gephyrocapsa oceanica* [$>6.5 \mu\text{m}$]) is at BID of 294.71 mbsf and between sapropels 944 and 943. Sapropel 944 at 301.67 mbsf corresponds to i-cycle 148 at 1.524 Ma and sapropel 943 at 284.01 mbsf corresponds to i-cycle 140 at 1.449 Ma. Datum 12 (FO acme of *Pseudoemiliana lacunosa*) is at BID of 269.73 mbsf and between sapropel 942 at 270.25 mbsf (i-cycle 132 at 1.376 Ma) and sapropel 941 at 267.08 mbsf (i-cycle 130 at 1.356 Ma).

In the upper Pleistocene sediments, the sapropel distribution is complete. As for Sites 976 and 977, the uppermost sapropel stratigraphic distribution is well correlated to the sequence of "S" sapropels described by Cita et al. (1977) for the eastern Mediterranean. Datum 3 (FO of *Emiliana huxleyi*) is at a BID of 58.02 mbsf and occurs between sapropel 914 (i-cycle 30 at 0.331 Ma) at 71.31 mbsf and sapropel 913 (i-cycle 24 at 0.262 Ma) at 55.80 mbsf. The sapropel 901 is correlated to i-cycle 2 at 8 Ka. Without oxygen isotope records, the stratigraphic position of sapropels above Datum 1 (FO *E. huxleyi* > *Gephyrocapsa* spp.) are more difficult to fix.

Sapropel Summary

A summary of the different sapropels recorded at all sites is presented in Figure 7 (Leg 161 coding of Murat, Chap. 41, this volume) and in Figure 8 (insolation cycle coding of Lourens et al., 1996a). Correlation of sapropels to the insolation cycles was supported by the oxygen isotope records recorded at Sites 975, 976, and 977. Figure 9 presents the oxygen isotopic events of these three sites and calcareous nannofossil datum ages calculated according to the sapropel chronology. The position of sapropels on the oxygen isotope curves at Site 975 is indicated in Pierre et al. (Chap. 38, this volume) and, for Sites 976 and 977, in von Grafenstein et al. (Chap. 37, this volume).

In general, strong sapropel TOC contents correspond to high-amplitude insolation maxima in the La90_(1,1) insolation curve. Low sapropel TOC contents correlate to intervals without marked insolation differences. In the Pleistocene interval, 88 insolation cycles (one cycle includes a minimum and a maximum in insolation intensity) are defined according to the astronomical insolation curve (Lourens et al., 1996a). Of this number, 68 cycles were observed in the western Mediterranean sites (Fig. 10). These calibrations show precisely when and which insolation cycles have developed sapropel layers. It is evident from Figure 7 that most of the Pleistocene insolation cycles correspond to sapropel development in the western Mediterranean. High-amplitude insolation maxima in Pleistocene sediments are al-

Table 10. Astronomical ages of biostratigraphic datums in Hole 979A, as indicated in Figure 6.

Hole 979A			
Event	Biostratigraphic Datum	Core, section, interval (cm)	Depth (mbsf)
1. FO	<i>Emiliana huxleyi</i> > <i>Gephyrocapsa</i> spp.	3H-4, 70; 3H-3, 120	16.20-15.20
2. FcO	<i>Emiliana huxleyi</i>	6H-4, 86; 6H-3, 121	44.89-43.71
3. FO	<i>Emiliana huxleyi</i>	7H-7, 20; 7H-6, 120	58.29-57.75
4. LO	<i>Pseudoemiliana lacunosa</i>	11H-3, 121; 11H-2, 120	91.21-89.70
5. LO	<i>Pseudoemiliana lacunosa lacunosa</i> (>7)	12H-2, 67; 11H-CC	97.87-93.62
6. LO acme	<i>Pseudoemiliana lacunosa</i>	20X-2, 120; 20X-1, 123	169.80-168.33
7. LO	<i>Crenalithus asanoi</i> (cir.; >6.5)	21X-1, 121; 20X-CC	178.01-176.17
8. FO	<i>Gephyrocapsa omega</i> (>4)	24X-3, 120; 24X-2, 120	209.20-208.40
9. FO	<i>Crenalithus asanoi</i> (cir.; >6.5)	27X-4, 120; 27X-3, 120	239.19-237.69
10. LO	<i>Gephyrocapsa</i> spp. (>6.5)	29X-2, 120; 28X-CC	255.56-253.20
11b LO	<i>Helicosphaera sellii</i>	29X-2, 120; 28X-CC	255.56-253.20
11. LcO	<i>Helicosphaera sellii</i>	29X-4, 120; 29X-4, 90	258.56-258.26
12. FO acme	<i>Pseudoemiliana lacunosa</i>	30X-6, 63; 30X-5, 120	270.20-269.27
13. FO	<i>Gephyrocapsa oceanica</i> (>6.5)	33X-3, 95; 33X-2, 121	295.33-294.09
14. FOs	<i>Gephyrocapsa caribbeanica</i> (>6.5) and <i>Gephyrocapsa oceanica</i> (>6.3)	33X-6, 119; 33X-5, 119	299.52-298.02
15. FO	<i>Gephyrocapsa oceanica</i> (>5.5)	34X-6, 94; 34X-5, 118	309.75-308.49
16. FO	<i>Gephyrocapsa</i> spp. (>5)	36X-2, 120; 36X-1, 121	323.68-322.31
17. LO	<i>Calcidiscus macintyreii</i> (cir., >11)	36X-3, 57-36X-2, 126	324.55-323.68
18. FO	<i>Gephyrocapsa oceanica</i> (>4)	37X-CC; 37X-7, 23	340.77-339.31
18b FO	<i>Gephyrocapsa caribbeanica</i> (>4)	38X-2, 120; 37X-CC	342.62-340.77
19. LO's	<i>Discoaster brouweri</i> and <i>Discoaster triradiatus</i>	44X-1, 120; 43X-CC	399.30-398.09
20. FO	<i>Globorotalia inflata</i> (Planktonic foraminifer datum)	47X-2, 46; 46X-CC	428.19-427.47

Note: LO = last occurrence, FO = first occurrence, LcO = last consistent occurrence, FcO = first consistent occurrence.

Table 11. Astronomical ages of biostratigraphic datums in Hole 979A as indicated in Figure 6.

Hole 979A			
Event	Biostratigraphic datum	Age (Ma)	Depth (mbsf)
1. FO	<i>Emiliana huxleyi</i> > <i>Gephyrocapsa</i> spp.	0.071	15.70
2. FcO	<i>Emiliana huxleyi</i>	0.218	44.30
3. FO	<i>Emiliana huxleyi</i>	0.274	58.02
4. LO	<i>Pseudoemiliana lacunosa</i>	0.410	90.45
5. LO	<i>Pseudoemiliana lacunosa lacunosa</i> (>7)	0.428	95.74
6. LO acme	<i>Pseudoemiliana lacunosa</i>	0.740	169.06
7. LO	<i>Crenalithus asanoi</i> (cir.; >6.5)	0.779	177.09
8. FO	<i>Gephyrocapsa omega</i> (>4)	0.962	208.80
9. FO	<i>Crenalithus asanoi</i> (cir.; >6.5)	1.126	238.44
10. LO	<i>Gephyrocapsa</i> spp. (>6.5)	1.246	254.43
11b LO	<i>Helicosphaera sellii</i>	1.246	254.43
11. LcO	<i>Helicosphaera sellii</i>	1.274	258.41
12. FO acme	<i>Pseudoemiliana lacunosa</i>	1.370	269.73
13. FO	<i>Gephyrocapsa oceanica</i> (>6.5)	1.494	294.71
14. FO	<i>Gephyrocapsa caribbeanica</i> (>6.5) and <i>Gephyrocapsa oceanica</i> (>6.3)	1.516	298.77
15. FO	<i>Gephyrocapsa oceanica</i> (>5.5)	1.566	309.12
16. FO	<i>Gephyrocapsa</i> spp. (>5)	1.625	322.99
17. LO	<i>Calcidiscus macintyreii</i> (cir., >11)	1.632	324.11
18. FO	<i>Gephyrocapsa oceanica</i> (>4)	1.719	340.04
18b FO	<i>Gephyrocapsa caribbeanica</i> (>4)	1.726	341.69
19. LO	<i>Discoaster brouweri</i> and <i>Discoaster triradiatus</i>	1.954	398.67
20. FO	<i>Globorotalia inflata</i> (Planktonic foraminifer datum)	2.090	427.83

Note: LO = last occurrence, FO = first occurrence, LcO = last consistent occurrence, FcO = first consistent occurrence.

ways correlated to a sapropel. Exceptions are in i-cycles 26 and 118, where no sapropels were observed at any sites.

Lower Pleistocene sapropel records (i-cycles 176 to 90) in the western Mediterranean (Sites 974 and 975) are very similar to land section records in the eastern Mediterranean (Vrica and Singa sections). Small-scale clusters, and cyclic alternation of distinct and less distinct sapropels, described by Hilgen (1991) in Southern Italy can be identified in lower Pleistocene sediments. Correlation of the sapropel distribution patterns to the insolation curve provide accurate calibration of sapropels.

Middle-upper Pleistocene sapropel records (i-cycles 88 to 2) are not complete at Sites 974 and 975. In contrast, Sites 976, 977, and

979, located further west, present a more complete middle-upper Pleistocene sapropel record. Several small-scale clusters of sapropels are identified in this time interval and are correlated to high-amplitude insolation maxima. In uppermost Pleistocene intervals, sapropel distribution patterns are very similar to sapropel successions described in eastern Mediterranean deep-sea cores. Most of the "S" sapropels (12 cycles from i-cycles 46 to 2) defined in the eastern Mediterranean were observed in the western Mediterranean; thus, similar paleoceanographic gradients occurred on each side of the Sicily sill during Pleistocene Epoch. Water exchanges from the western Mediterranean to the Atlantic during Pleistocene climatic changes may have been important to preserve the paleoceanographic gradients necessary to initiate the development of sapropels in the western Mediterranean. Detailed paleoceanographic evolution and history of sapropel formation are given by Murat (Chap. 41, this volume) and Dooze et al. (Chap. 39, this volume).

BIOHORIZONS

As indicated above, the Pleistocene biostratigraphic framework for this study is the succession of 20 calcareous nannofossil biohorizons indicated in Figures 2–6 and summarized in Figure 10 and Table 12. Some of these datums are included in the nannofossil zonations of Martini (1971) and Gartner (1977). Additional, reliable biohorizons are proposed to subdivide further the Pleistocene interval. All biohorizon ages, summarized in Table 12, are calculated according to a new, more accurate, and precise time scale based on the astronomical insolation cycles according to Laskar et al.'s solution (1993). Included with each biohorizon description are references to relevant biostratigraphic studies in the Mediterranean, Atlantic Ocean, and Pacific Ocean, where nannofossil datum ages were estimated by calibration to oxygen isotope stratigraphy or astronomical templates.

Datum 18

***FO of Gephyrocapsa oceanica* (>4 μ m) and *FO of Gephyrocapsa caribbeanica* (>4 μ m)**

The evolutionary trends observed in genus *Gephyrocapsa* within the early Pleistocene have been used in numerous studies to provide

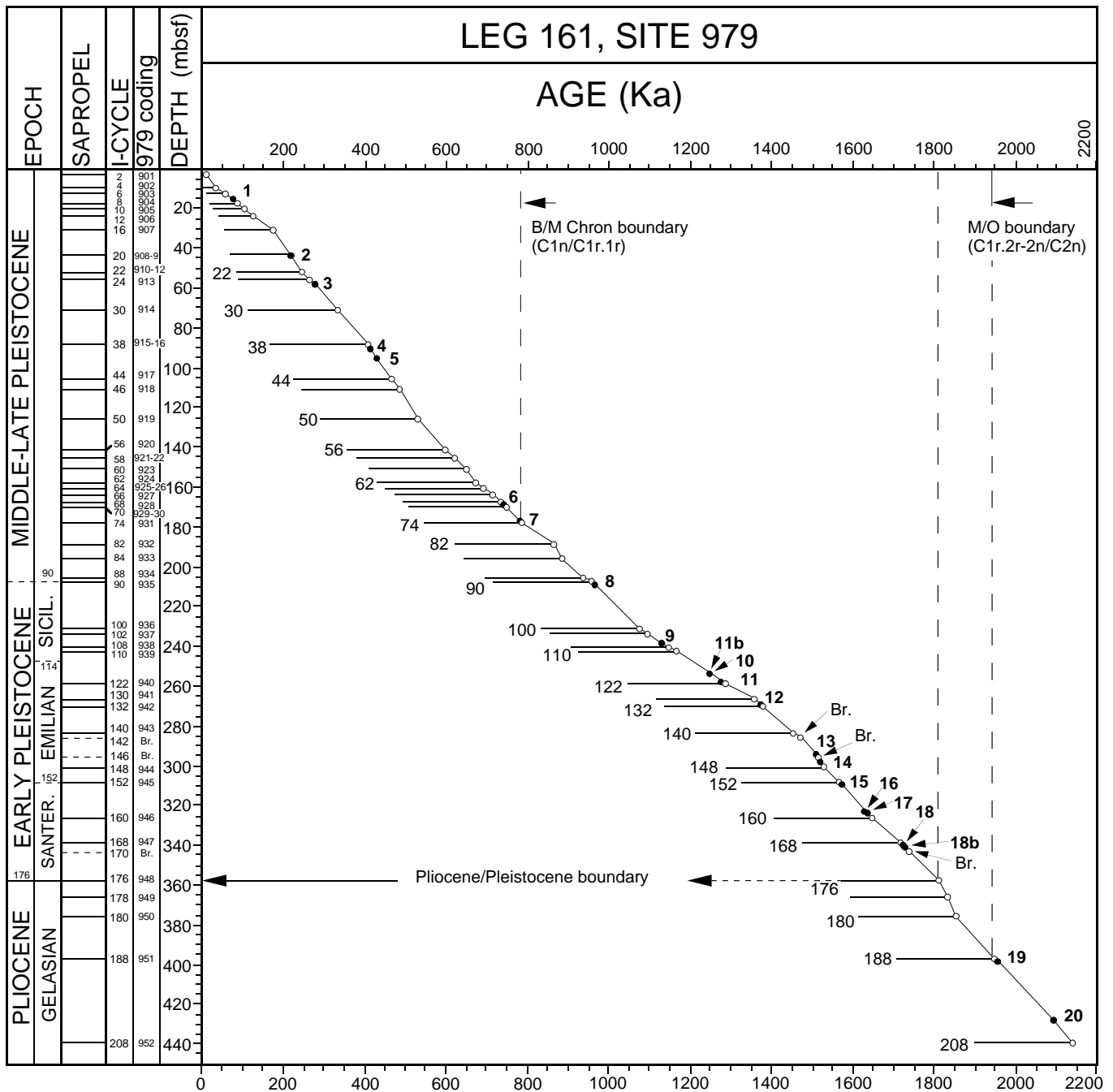


Figure 6. Age-depth plot. Calibration of sapropels at Site 979 with the insolation cycles. Position and age of calcareous nannofossil events (black dots: datums 1–19) are from Tables 10 and 11. Sapropels (45 white dots) are numbered (Site 979 coding described by Murat, Chap. 41, this volume) and correlated to the insolation cycle (i-cycle). Ages of i-cycles are indicated in Table 1. Br. = *Braudosphaera bigelowii* bloom.

biostratigraphic events to zone this period of time (Rio, 1982; Rio et al., 1990a; Raffi et al., 1993). The detailed study of *Gephyrocapsa* conducted by Matsuoka and Okada (1990) gave an overview of the changes in placolith size, central opening diameters, and inclination of the bridge through time. The first nannofossil event to occur at the base of the Pleistocene and used to approximate the Pliocene/Pleistocene boundary is the first occurrence of medium (>4 μm) *Gephyrocapsa*. This boundary is defined as the top of the sapropel “e” (i-cycle 176 at 1.808 Ma) at the type section of Vrica (Italy) and an age of 1.806 Ma has been calculated by Lourens et al. (1996a).

Gephyrocapsa >4 μm and <5.5 μm in size with an open central area were labeled *Gephyrocapsa oceanica* s.l. by Rio et al. (1990a). *Gephyrocapsa* >4 μm with a very small central opening are labeled *Gephyrocapsa caribbeanica* by Sato et al. (1991). Matsuoka and Okada (1990) in their morphometric study included both types of *Gephyrocapsa* in one morphogroup, *Gephyrocapsa* sp. B. According to Sato et al. (1991), *Gephyrocapsa caribbeanica* (>4 μm) occurs earlier than *Gephyrocapsa oceanica* (>4 μm). They considered the FO of *G. caribbeanica* as the first Pleistocene datum. In our study of sediments from Hole 975C and from Hole 979A, these bioevents were

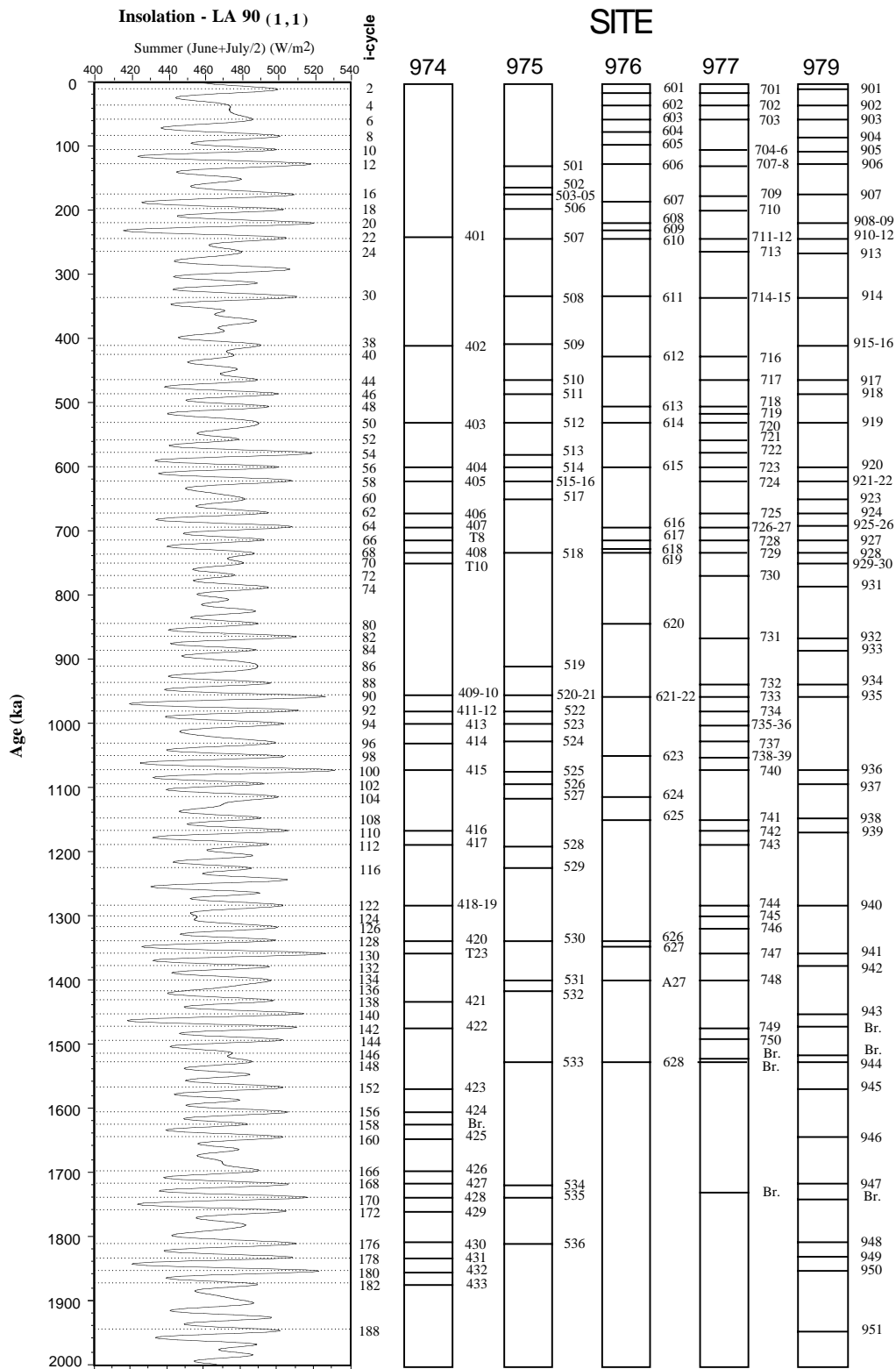


Figure 7. Calibration of late Pliocene and early Pleistocene sapropels at ODP Sites 974 to 977, and 979 to the La90_(1,1) (Laskar et al., 1993) summer insolation curve. The coding of sapropels is from Murat (Chap. 41, this volume). The coding of insolation cycles (i-cycle) indicated to the right side of the insolation curve is from Lourens et al. (1996a). Br. = *Braarudosphaera bigelowii* layers.

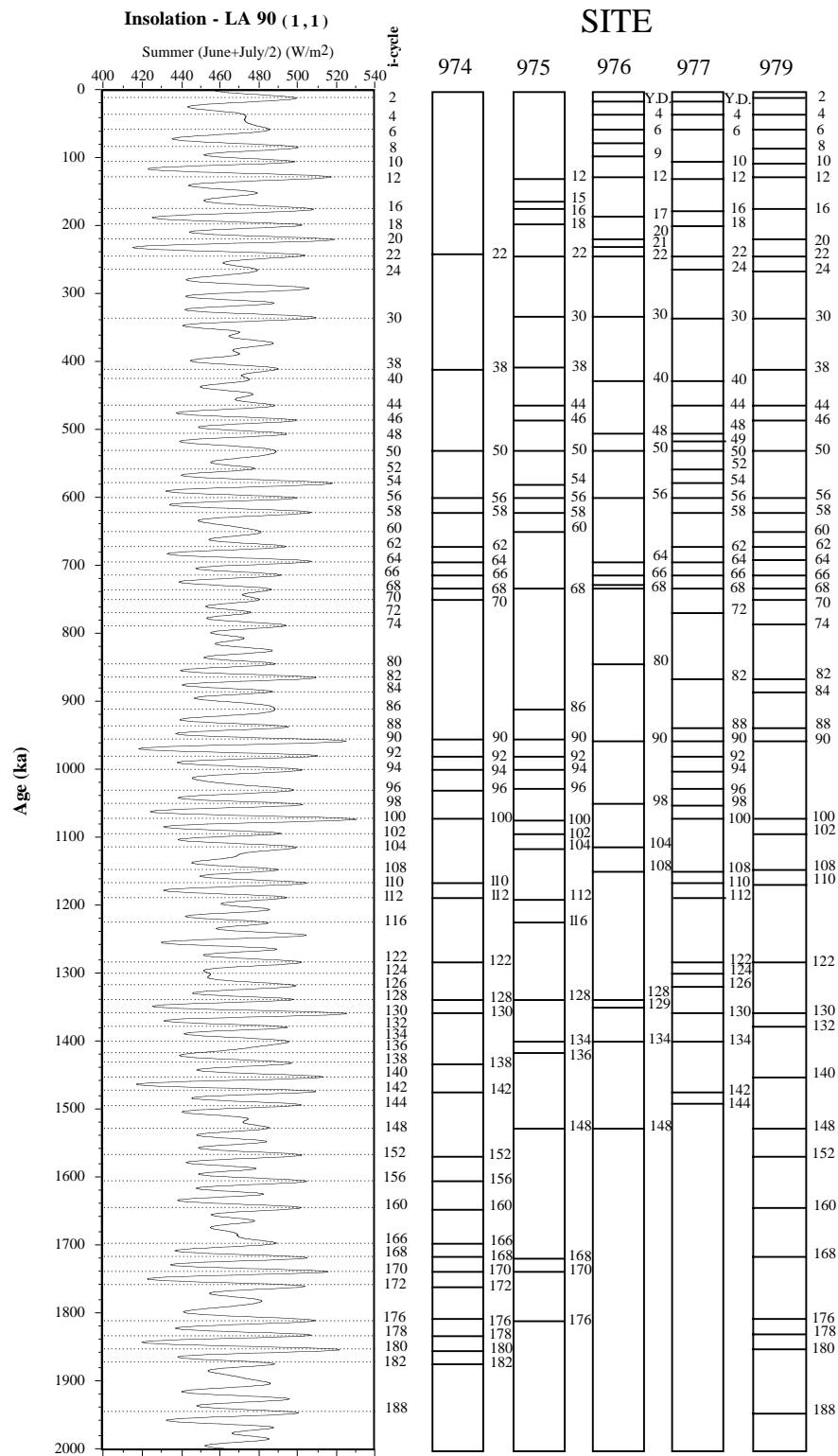
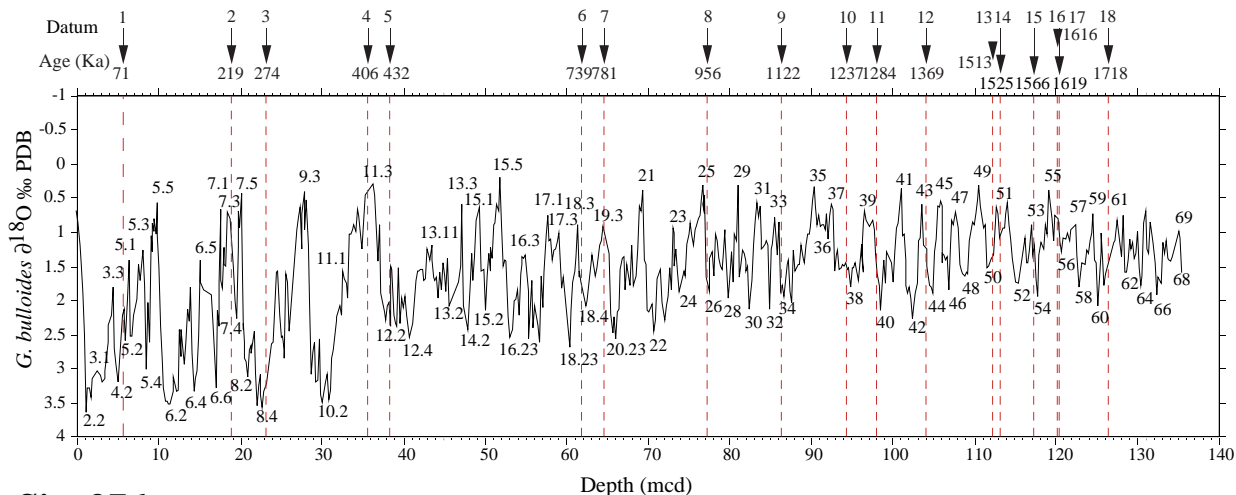
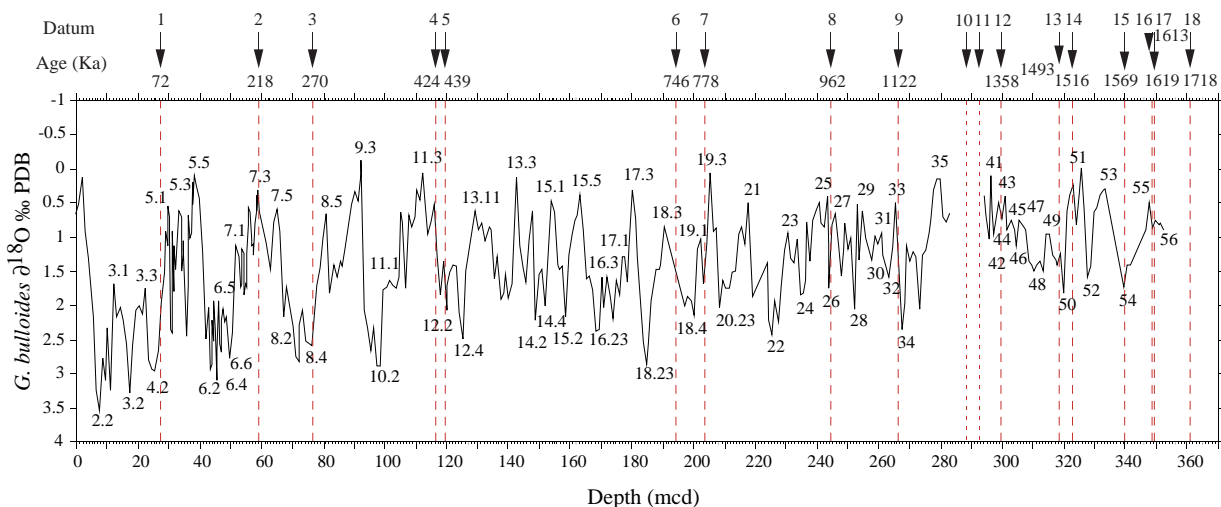


Figure 8. Calibration of late Pliocene and early Pleistocene sapropels at ODP Sites 974 to 977, and 979 to the La90_(1,1) (Laskar et al., 1993) summer insolation curve. The coding of insolation cycles (i-cycle) indicated to the right side of the insolation curve is from Lourens et al. (1996a). Coding of sapropels indicated in Figure 7 is replaced herein by the insolation cycle coding of Lourens et al. (1996a) according to correlations indicated in Figures 2–6.

Site 975



Site 976



Site 977

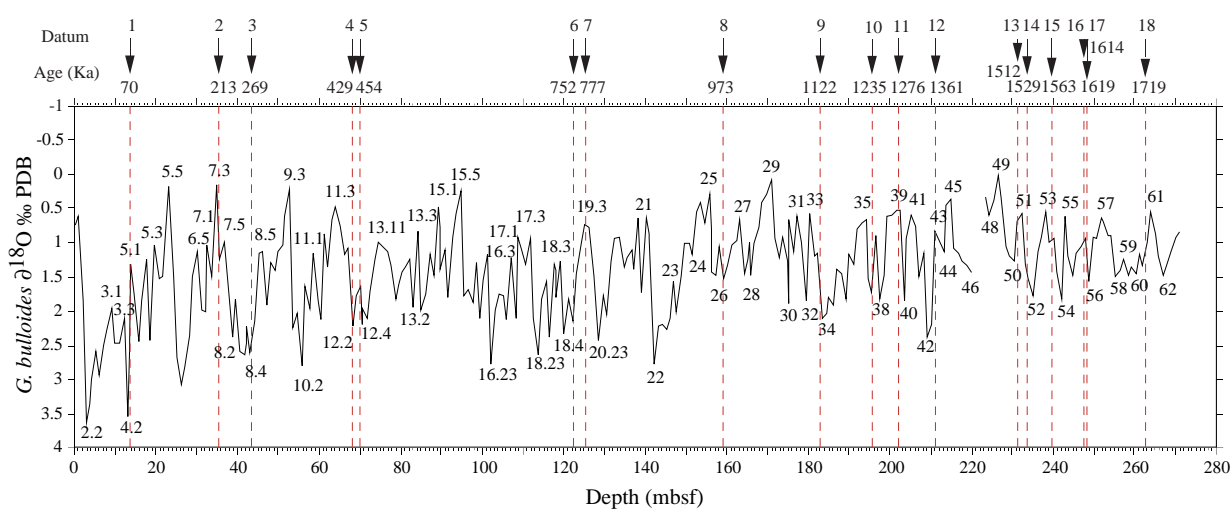


Figure 9. Oxygen isotope records from *G. bulloides* vs. depth from Sites 975, 976, and 977. Position and age of calcareous nanofossil biostratigraphic datums (Table 12) are linked to the oxygen isotopic events.

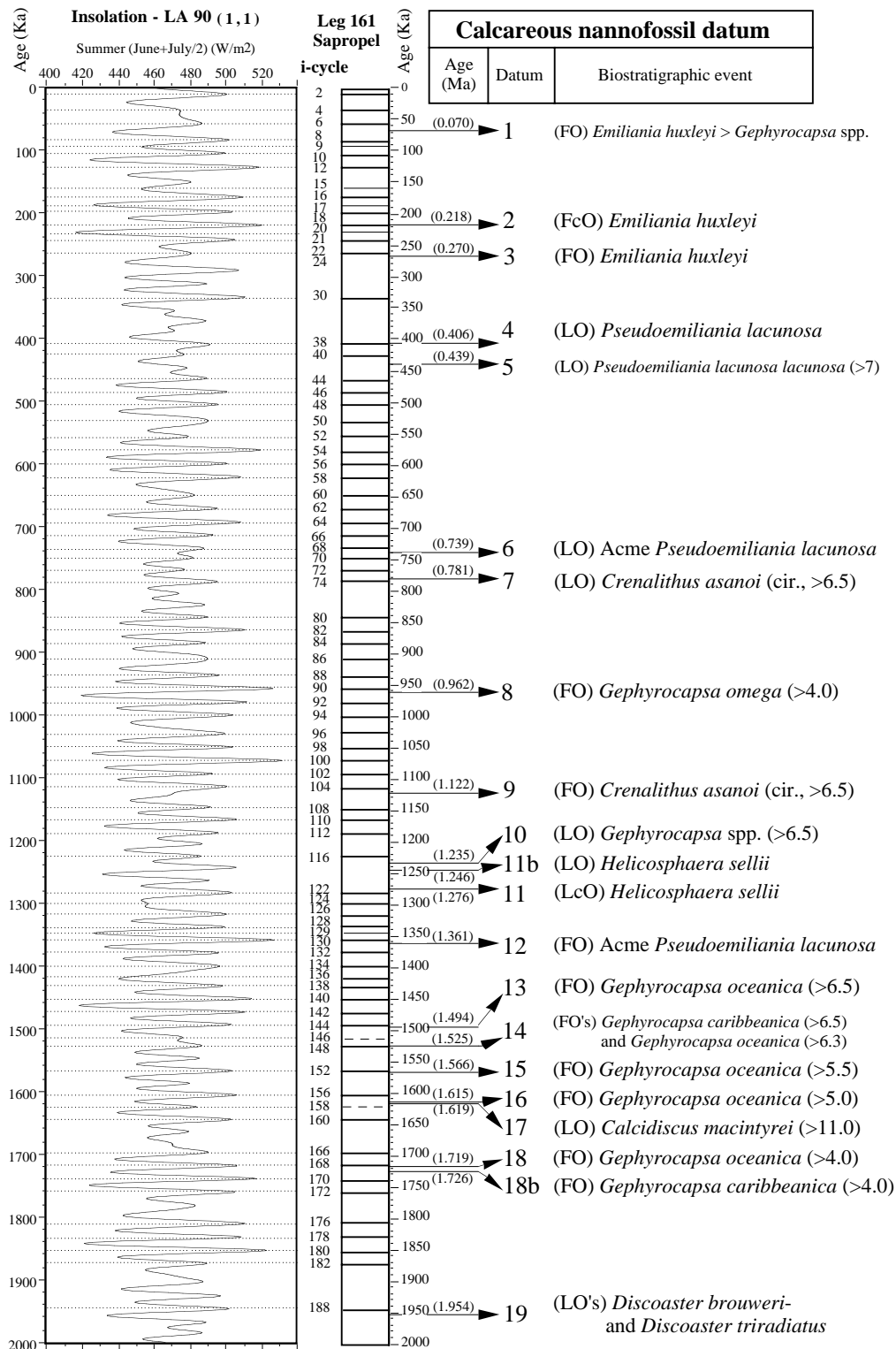


Figure 10. Calibration of late Pliocene and early Pleistocene calcareous nannofossil datums to the La90_(1,1) (Laskar et al., 1993) summer insolation curve and to Leg 161 sapropels. Calcareous nannofossil datum ages are from Table 12 (best estimate of the datum age). The coding of insolation cycles (i-cycle) indicated to the right side of the insolation curve is from Lourens et al. (1996a). The column in the middle includes all sapropels recovered at all Leg 161 Sites.

Table 12. ODP sites best used to estimate ages of calcareous nannofossil datums, based on data from Sites 974 to 977, and 979.

Datums	Calcareous nannofossil events	Best estimate of the datum age (Ma)	Best site of the datum position	Site 974 age (Ma)	Site 975 age (Ma)	Site 976 age (Ma)	Site 977 age (Ma)	Site 979 age (Ma)
1	FO <i>Emiliana huxleyi</i> > <i>Gephyrocapsa</i> spp.	0.070	977	0.071	0.071	0.072	0.070	0.071
2	FcO <i>Emiliana huxleyi</i>	0.218	976	0.218	0.219	0.218	0.213	0.218
3	FO <i>Emiliana huxleyi</i>	0.270	976	0.274	0.274	0.270	0.269	0.274
4	LO <i>Pseudoemiliana lacunosa</i>	0.406	975	0.408	0.406	0.424	0.429	0.410
5	LO <i>Pseudoemiliana lacunosa lacunosa</i> (>7)	0.439	976	0.430	0.432	0.439	0.454	0.428
6	LO acme <i>Pseudoemiliana lacunosa</i>	0.739	975	0.751	0.739	0.746	0.752	0.740
7	LO <i>Crenalithus asanoi</i>	0.781	975	0.781	0.781	0.778	0.777	0.779
8	FO <i>Gephyrocapsa omega</i> (>4)	0.962	976	0.964	0.956	0.962	0.973	0.962
9	FO <i>Crenalithus asanoi</i>	1.122	977	1.122	1.122	1.122	1.122	1.126
10	LO <i>Gephyrocapsa</i> spp. (>6.5)	1.235	977	1.243	1.237		1.235	1.246
11b	LO <i>Helicosphaera sellii</i>	1.246	979					1.246
11	LcO <i>Helicosphaera sellii</i>	1.276	977	1.272	1.284		1.276	1.274
12	FO acme <i>Pseudoemiliana lacunosa</i>	1.361	977	1.359	1.369	1.358	1.361	1.370
13	FO <i>Gephyrocapsa oceanica</i> (>6.5 μ m)	1.494	979	1.498	1.513	1.493	1.512	1.494
14	FO <i>Gephyrocapsa caribbeanica</i> (>6.5) - <i>Gephyrocapsa oceanica</i> (>6.3)	1.525	975	1.521	1.525	1.516	1.529	1.516
15	FO <i>Gephyrocapsa oceanica</i> (>5.5 μ m)	1.566	974	1.566	1.566	1.569	1.563	1.566
16	FO <i>Gephyrocapsa</i> spp. (>5)	1.615	974	1.615	1.616	1.613	1.614	1.625
17	LO <i>Calcidiscus macintyreii</i> (>11)	1.619	974	1.619	1.619	1.619	1.619	1.632
18	FO <i>Gephyrocapsa oceanica</i> (>4)	1.719	979	1.721	1.718	1.718	1.719	1.719
18b	FO <i>Gephyrocapsa caribbeanica</i> (>4)	1.726	979		1.720			1.726
19	LO <i>Discoaster brouweri</i>	1.954		1.954	1.954			1.954

Note: Ages refer to the midpoints between lower and upper limits of the placement of the datum.

separated. In Hole 975C, the FO of *Gephyrocapsa caribbeanica* (>4 μ m) occurs 20 cm (Table 4) below the FO of *Gephyrocapsa oceanica* (>4 μ m). In Hole 979A, the FO of *Gephyrocapsa caribbeanica* (>4 μ m) occurs ~146 cm (Tables 10 and 11) below the FO of *Gephyrocapsa oceanica* (>4 μ m). In general, without high sample resolution and high sedimentation rates, these two bioevents cannot be differentiated.

The age of the FO of medium *Gephyrocapsa* (>4 μ m) given in the literature changes according to the time scales used. Sprovieri (1993a, 1993b) found the FO of *Gephyrocapsa oceanica* s.l. at 1.75 Ma in the eastern Mediterranean by using the time scale of Shackleton et al. (1990). Raffi et al. (1993), using the same time scale, reported this bioevent at 1.67 Ma in the Equatorial Pacific (Site 677) and at 1.70 Ma in the North Atlantic (Site 607). Rio et al. (1997) reported the FO of *Gephyrocapsa oceanica* s.l. between sapropel "f" (= i-cycle 170 at 1.736 Ma) and sapropel "h" (= i-cycle 168 at 1.715 Ma) at the Vrica type section. Lourens et al. (1996a) placed the same event in the i-cycle 167, above sapropel "h" (i-cycle 168), and dated it at 1.71 Ma. This discrepancy in the stratigraphic position of *Gephyrocapsa oceanica* s.l. at the type section of Vrica probably is a result of mislabeling sapropel "h." Our study confirms the stratigraphic position of *Gephyrocapsa oceanica* s.l. reported by Rio et al. (1997) in the eastern Mediterranean. In the western Mediterranean, the FO of *Gephyrocapsa oceanica* (>4 μ m) also occurs between i-cycle 170 and i-cycle 168.

Site 979 was selected among the three Leg 161 sites with lowermost Pleistocene sapropels (Sites 974, 975, and 979; Fig. 7) to define the age of the FO of *Gephyrocapsa oceanica* (>4 μ m; Table 12). At Site 979, this bioevent is delineated by sapropel 947 (i-cycle 168) and by a *Braarudosphaera bigelowii* ooze (i-cycle 170; Fig. 6). An age of 1.719 Ma has been calculated for the FO of *Gephyrocapsa oceanica* (>4 μ m) and an age of 1.726 Ma for the *Gephyrocapsa caribbeanica* (>4 μ m; datum 18b). At Site 974, these datums are delineated by two, thin sapropels (428 and 427; Fig. 7) with high TOC values, and by a high sampling resolution. At Site 975, these datums are also recorded between two sapropels (535 and 534; Fig. 7). On the oxygen isotope curves (Fig. 9), an age of 1.719 Ma fits between stage 60 and stage 61 (transition 60/61).

Datum 17

LO of Calcidiscus macintyreii (circular, >11.0 μ m)

The progressive placolith size decrease in the genus *Calcidiscus* is used as the second Pleistocene bioevent. Numerous biostratigraphic studies have used different placolith size concepts or ignore size in determining this datum. According to Backman and Shackleton (1983), the distinction between the size of the *Calcidiscus leptoporus* and *Calcidiscus macintyreii* is 10 μ m. Rio et al. (1990a, 1990b), following the concept of Backman and Shackleton (1983), also proposed using the same size distinction to place the LO of *Calcidiscus macintyreii* in the early Pleistocene. Fornaciari et al.'s (1990) biometric analyses determined that the appearance of *Calcidiscus macintyreii* is determined by specimens larger than 11 μ m. Following this study, Raffi and Flores (1995) used the 11- μ m size to split the two *Calcidiscus* species and also further restricted *Calcidiscus* species concepts. They assign to *Calcidiscus macintyreii* only forms larger than 11 μ m that have a circular outline. This distinction is very important (see "Paleontological Systematic Description" below) and the same species concept is used herein. Only the circular forms of *Calcidiscus* larger than 11 μ m and with more than 40 elements in the distal shield are used to define this datum.

As a result of these different concepts, age estimations for this extinction event have varied widely. Raffi et al. (1993) estimated, using the Shackleton et al. (1990) time scale, the LO *Calcidiscus macintyreii* at 1.597 Ma in the Equatorial Pacific (Site 677) and at 1.640 Ma in the North Atlantic (Site 607). They also placed the LO of *Calcidiscus macintyreii* at Site 607 at the beginning of $\delta^{18}\text{O}$ stage 57. Stage 57 is in the astronomical time scale between i-cycle 160 (1.642 Ma) and 158 (1.622 Ma). Berger et al. (1994) proposed an age of 1.627 Ma (± 0.025) for the LO of *Calcidiscus macintyreii* at Site 806 in the western Equatorial Pacific. This age was obtained by tuning their oxygen isotope and GRAPE (gamma-ray attenuation porosity evaluator) records to an orbital template based on the astronomical solution of Berger and Loutre (1991). In the eastern Mediterranean, Sprovieri (1993a, 1993b) indicated an age of 1.62 Ma by calibration to Shackleton et al.'s (1990) time scale. Lourens et al. (1996a) placed the LO of *Calcidiscus macintyreii* at 1.67 Ma in the i-cycle 164. At Singa/Vri-

ca sections, the LO of *Calcidiscus macintyreii* is between sapropels "C9/h" and C10/n, which correspond respectively to i-cycle 168 at 1.715 Ma and to i-cycle 160 at 1.642 Ma (Lourens et al., 1996a). Lourens et al. (1998) placed the eastern Mediterranean LO of *Calcidiscus macintyreii* at the Vrica section at 1.671 Ma, at Site 967 (ODP Leg 160) at 1.673 Ma, and in Hole 969D (ODP Leg 160) at 1.663 Ma. By comparing the different studies, ages of the LO of *Calcidiscus macintyreii* do not correspond between the eastern Mediterranean and the North Atlantic. In the western Mediterranean Site 974, the LO *Calcidiscus macintyreii* is situated above i-cycle 160. Detailed analyses and high sampling resolution have demonstrated the consistent occurrence of rare specimens just above the i-cycle 160 and the same age (1.619 Ma) has been calculated at Sites 974, 975, 976 and 977 (Table 12; Figure 9). Oxygen isotopic events (Fig. 9) were used to calculate ages of the LO of *Calcidiscus macintyreii* at Sites 975, 976, and 977. Because two thin sapropels (160 and 156) with high TOC contents, along with high sampling resolution, were present at Site 974, this site was selected to calculate precisely the LO of *Calcidiscus macintyreii* (>11 μm). An age of 1.619 Ma is calculated for this datum, which places the LO of *Calcidiscus macintyreii* in the upper part of $\delta^{18}\text{O}$ stage 56 (Fig. 9).

Datum 16

FO of Gephyrocapsa spp. (>5 μm)

In the *Gephyrocapsa morphometric* classification established by Matsuoka and Okada (1989) and by Raffi et al. (1993), different length criteria are used to differentiate small, medium, and large *Gephyrocapsa*. Generally, the following classification is adopted:

- Very small forms: *Gephyrocapsa* spp. (<2.5 μm),
- Small forms: *Gephyrocapsa* spp. (2.5–4.0 μm),
- Medium forms: *Gephyrocapsa* spp. (>4.0–5.5 μm),
- Large forms: *Gephyrocapsa* spp. (>5.5 μm).

This *Gephyrocapsa* length classification does not correspond to general coccolith size concepts (very small = 1–3 μm , small = 3–5 μm , medium = 5–8 μm , and large = 8–12 μm) (Young et al., 1997), but it is used in the *Gephyrocapsa* taxonomy to indicate the morphometric evolution within this group. Different *Gephyrocapsa* lengths have been used in the literature to separate the medium from large *Gephyrocapsa* forms: 5.0, 5.5, 6.0, and 6.5. Each length corresponds to a different step in the morphometric evolution of *Gephyrocapsa* and may be used as a datum. We measured four different lengths (μm): 4.0, 5.0, 5.5, and 6.5 (see datums 15 and 14 below).

Matsuoka and Okada (1989) used 5.0 μm to differentiate the medium *Gephyrocapsa* from the large ones. The FO of *Gephyrocapsa* (>5 μm) occurs close to the level of the LO of *Calcidiscus macintyreii* (>11 μm). At all Leg 161 sites, the occurrence of *Gephyrocapsa* (>5 μm) is observed between 3 and 7 k.y. (Table 12), above the LO of *C. macintyreii*. This bioevent (a first occurrence) is especially useful to determine the exact stratigraphic position of the last occurrence of *C. macintyreii* when the latter species is reworked. Based on Site 974, an age of 1.615 Ma is assigned to the FO of *Gephyrocapsa* (>5 μm) and correlates to the $\delta^{18}\text{O}$ stage 56 (1.625 Ma). As for the *C. macintyreii* datum, the FO of *Gephyrocapsa* (>5 μm) is situated between i-cycle 160 (1.642 Ma) and i-cycle 156 (1.603 Ma). An age of 1.615 Ma corresponds to i-cycle 157.

Datum 15

FO of Gephyrocapsa oceanica (>5.5 μm)

As indicated by Raffi et al. (1993), this biostratigraphic event reflects one episode in the morphometric evolution of *Gephyrocapsa*.

Using Shackleton et al.'s (1990) time scale, Raffi et al. (1993) estimated the age of this bioevent at 1.457 Ma in the Equatorial Pacific (Site 677) and at 1.479 Ma in the North Atlantic (Site 607). Using the same time scale, Sprovieri (1993a, 1993b) obtained an age of 1.50 Ma for this bioevent in the eastern Mediterranean. Based on outcrop sections in Italy, Lourens et al. (1996a) placed the FO of *Gephyrocapsa* (>5.5 μm) in i-cycle 157 and estimated an age of 1.61 Ma. Lourens et al. (1998) placed the FO of *Gephyrocapsa* (>5.5 μm) at Vrica at 1.608 Ma (in i-cycle 156), at Site 967 at 1.616 Ma (in i-cycle 157), and at Hole 969D at 1.626 Ma (in i-cycle 158). These ages do not correspond to the biostratigraphic results published in Lourens et al. (1996b). In that paper, Lourens et al. (1996b) indicated that the FO of *Gephyrocapsa* spp. (>5.5 μm) in the Vrica section (Italy) occurs close to the sapropel "p" and in the Singa section near the sapropel "C12." Sapropels "p" and "C12" correspond to the same i-cycle 152 at 1.564 Ma. At Sites 974 and 979 in the western Mediterranean, the same stratigraphic relationship is observed. At Site 974, the FO of *Gephyrocapsa oceanica* (>5.5 μm) occurs shortly at the base of the thin sapropel 423 (i-cycle 152) (Fig. 2); at Site 979, this bioevent is observed within the lower part of the thick sapropel 945 (i-cycle 152) (Fig. 6). Based on Site 974, an age of 1.566 Ma is assigned to this event, which places the FO of *Gephyrocapsa oceanica* (>5.5 μm) at the base of the sapropel from i-cycle 152 (1.564 Ma). An age of 1.566 Ma corresponds to the transition between $\delta^{18}\text{O}$ stages 54/53 (Fig. 9).

Datum 14

FO of Gephyrocapsa oceanica (>6.3 μm) and FO of Gephyrocapsa caribbeanica (>6.5 μm)

The stratigraphic position of the FO of *Gephyrocapsa oceanica* (>6.0 μm) was not determined in this study. This morphometric distinction in *Gephyrocapsa* was used as a datum by Sato et al. (1991) and by Takayama (1993). Takayama (in Berger et al., 1994), at Site 806 in the western Equatorial Pacific, estimated an age of 1.515 Ma (± 0.025) for this datum by tuning their oxygen isotope record to an orbital template based on the astronomical solution of Berger and Loutre (1991).

The FOs of *G. caribbeanica* (>6.5 μm) and *G. oceanica* (>6.5 μm) are the last two morphometric size increases used to zone the early Pleistocene and are also used as biostratigraphic datums in several studies. We observed that the FO of *Gephyrocapsa caribbeanica* (>6.5 μm) occurs one insolation cycle before the first occurrence of *Gephyrocapsa oceanica* (>6.5 μm). However, we observed that the first occurrences of *Gephyrocapsa caribbeanica* (>6.5 μm) and *Gephyrocapsa oceanica* (>6.3 μm) are coincident. *Gephyrocapsa caribbeanica* (>6.5 μm) is more difficult to find, but together with *Gephyrocapsa oceanica* (>6.3 μm), these two bioevents provide a useful biohorizon.

This biohorizon is placed at the level of i-cycle 148 (1.524 Ma). A sapropel is present at Site 975 (533), at Site 976 (628), and at Site 979 (944), which allows precise placement of this datum. Based on Site 975, we calculated an age of 1.525 Ma for this datum. This age corresponds by correlation to the $\delta^{18}\text{O}$ stage to the Stages 51 (Fig. 9).

Datum 13

FO of Gephyrocapsa oceanica (>6.5 μm)

At Sites 974, 976, and 979, the FO of *Gephyrocapsa oceanica* (>6.5 μm) occurs in i-cycle 144 (1.490 Ma). At Sites 975 and 977, very rare specimens of *Gephyrocapsa oceanica* (>6.5 μm) were observed in i-cycle 146 (1.511 Ma). An age of 1.494 Ma is determined for the FO of *Gephyrocapsa oceanica* (>6.5 μm), based on the data from Site 979 (Table 12). By correlation to the oxygen isotope

stratigraphy (Fig. 9), this datum is correlated to the upper part of oxygen isotope event 50. An age of 1.513 Ma (occurrence of very rare specimens of *Gephyrocapsa oceanica* [$>6.5 \mu\text{m}$]), calculated for this datum at Site 975 (Table 12), fits between the oxygen isotope stage 50 and 51 (transition 50/51; Fig. 9).

Datum 12

FO acme of *Pseudoemiliana lacunosa*

We propose this datum to subdivide further the large *Gephyrocapsa* spp. ($>6.5 \mu\text{m}$) interval. This bioevent is characterized by a marked increase in *Pseudoemiliana* populations and corresponds to a change in abundance from common (1 specimen per 2–10 fields of view) to abundant (1–10 specimens per field of view). This acme is recorded in i-cycle 130. The i-cycle 130 (1.356 Ma) is recognized at Sites 974, 977, and 979 by the presence of a thick sapropel (respectively T23, 747, and 941; Fig. 7). Based on Site 977, an age of 1.361 Ma is assigned for the onset of the acme of *Pseudoemiliana lacunosa*, which places this bioevent within the high-amplitude maximum of i-cycle 130. By calibration to the oxygen isotope stratigraphy, this datum is correlated to the stage 43.

Datum 11

LcO of *Helicosphaera sellii*

The LO of *Helicosphaera sellii* is considered in various studies to be diachronous between biogeographic provinces. Careful examination of the stratigraphic position of the LO of *Helicosphaera sellii* and of the different time scales used is necessary to confirm this diachrony. Raffi et al. (1993), using Shackleton et al.'s (1990) time scale, reported the LO of *Helicosphaera sellii* just below the LO of *Gephyrocapsa* spp. ($>5.5 \mu\text{m}$) in the North Atlantic (Site 607). They estimated an age of 1.241 Ma for this datum. Raffi et al. (1993) determined an age of 1.470 Ma for this datum in the Equatorial Pacific (Site 677).

Lourens et al. (1994) reported that at the eastern Mediterranean section of Vrica, the LO of *Helicosphaera sellii* was above sapropel "v" (i-cycle 122 at 1.280 Ma) and between oxygen isotope stages 38 (1.246 Ma) and 36 (1.203 Ma). Lourens et al. (1996a) correlated this stratigraphic position to i-cycle 117–118 and estimated an age of 1.24 Ma for the LO of *Helicosphaera sellii*. At the Vrica section, the LO of *Helicosphaera sellii* is at the level of the LO of *Gephyrocapsa* spp. ($>5.5 \mu\text{m}$) and, therefore, both biostratigraphic datums have the same age of 1.24 Ma (i-cycle 117–118) in the table of Lourens et al. (1996a). Berggren et al. (1995) indicated an age of 1.22 Ma for the extinction of *Helicosphaera sellii* in mid-latitudes, based on the study of Rio et al. (1991) in the Tyrrhenian Sea. An age of 1.22 Ma corresponds to the oxygen isotope stage 37.

At Sites 974, 977, and 979, we also observed the LO of *Helicosphaera sellii* above the i-cycle 122 (sapropel "v" at the Vrica section) and below the LO of *Gephyrocapsa* spp. ($>6.5 \mu\text{m}$). Nevertheless, the exact stratigraphic position of the LO of *Helicosphaera sellii* is often affected by the presence of reworked specimens. In order to establish a consistent and correlative event, we used the last consistent occurrence of *Helicosphaera sellii*. This datum is between i-cycle 120 (1.261 Ma) and i-cycle 122 (1.280 Ma). Based on Site 977, an age of 1.276 Ma is determined for the LcO of *Helicosphaera sellii* by sapropel 744 (i-cycle 122). This chronological position corresponds in the oxygen isotope stratigraphy to stage 39. At Site 979, specimens of *Helicosphaera sellii* were recorded inconsistently above this level to the lowest occurrence of *Gephyrocapsa* spp. ($>6.5 \mu\text{m}$).

Datum 10

LO of *Gephyrocapsa* spp. ($>6.5 \mu\text{m}$)

The temporary disappearance of almost all *Gephyrocapsa* species larger than $4 \mu\text{m}$ at about 1.25 Ma has been observed worldwide in

Pleistocene sections. The quantitative morphometric analysis from Matsuoka and Okada (1989) indicates that large ($>5 \mu\text{m}$) forms of *Gephyrocapsa caribbeanica* and *Gephyrocapsa oceanica* have the same extinction level, but their sampling density was low (one sample about every 100 k.y.). Raffi et al. (1993), using the Shackleton et al.'s (1990) time scale, estimated the age of the LO of large *Gephyrocapsa* spp. ($>5.5 \mu\text{m}$) at 1.240 Ma in the Equatorial Pacific (Site 677) and at 1.227 Ma in the North Atlantic (Site 607). Shackleton et al. (1995), based on biostratigraphic data from Raffi and Flores (1995), estimated the age of the LO of large *Gephyrocapsa* spp. ($>5.5 \mu\text{m}$) at 1.24 Ma in the eastern Equatorial Pacific. Lourens et al. (1996a) estimate the same age of 1.24 Ma for this datum in the eastern Mediterranean. There is good agreement to place the LO of large *Gephyrocapsa* spp. ($>5.5 \mu\text{m}$) in the upper part of the oxygen isotope stage 38, but very rare specimens of *Gephyrocapsa* spp., smaller than $6.5 \mu\text{m}$, may be observed above this level. In contrast, forms larger than $6.5 \mu\text{m}$ are not recorded above this level. The age of 1.227 Ma estimated by Raffi et al. (1993) for the LO of *Gephyrocapsa* spp. ($>5.5 \mu\text{m}$) in the North Atlantic may reflect the LO of *Gephyrocapsa* spp. between 5.5 and $6.5 \mu\text{m}$. In the "small *Gephyrocapsa* Zone" defined by Gartner (1977) as the interval between the LO of *Helicosphaera sellii* and the highest level of dominantly small *Gephyrocapsa*, very rare forms of *Gephyrocapsa* spp. ($>5.5 - <6.0 \mu\text{m}$) may be observed within the *Crenalithus* populations.

We propose the use of $6.5 \mu\text{m}$ as the size limit to define this datum. The LO of *Gephyrocapsa* spp. ($>6.5 \mu\text{m}$) is situated in the lower part of i-cycle 118. Based on oxygen isotope record at Site 977, an age of 1.235 Ma is assigned to the LO of *Gephyrocapsa* spp. ($>6.5 \mu\text{m}$) (Table 12). This chronological position occurs in the stage 38.

Datum 9

FO of *Crenalithus asanoi* (circular, $>6.5 \mu\text{m}$)

Crenalithus asanoi (new combination, this paper) was first recognized by Takayama and Sato (1987) as *Reticulofenestra* sp. A (sub-elliptical forms) and as *Reticulofenestra* sp. B (circular forms). It was later formally described as *Reticulofenestra asanoi* by Sato and Takayama (1992). Matsuoka and Okada (1989) used the first occurrence of *Reticulofenestra* sp. A ($>6.5 \mu\text{m}$) to subdivide the "small *Gephyrocapsa* Zone." Sato et al. (1991) used the onset acme of *Crenalithus asanoi* (subcircular to circular forms) as a datum, but without a size indication. As indicated in their species description, they probably used $6 \mu\text{m}$ or more to separate the small and medium *Crenalithus* species (see "Paleontological Systematic Description" below—*Crenalithus* species concept). In the western Mediterranean, the onset of the acme of *Crenalithus asanoi* and the FO of *Crenalithus asanoi* ($>6.5 \mu\text{m}$) are also two very close, but distinct, bioevents. To have a consistent datum, we used the FO of *Crenalithus asanoi* ($>6.5 \mu\text{m}$). This datum is observed just above the onset of the acme of *Crenalithus japonicus* ($>5.0 - 6.5 \mu\text{m}$).

Matsuoka (in Berger et al., 1994) estimated the age of the FO of *Crenalithus asanoi* at 1.168 Ma (± 0.025) in the western Equatorial Pacific (Site 806) by calibration to the astronomical solution of Berger and Loutre (1991). At Sites 976, 977, and 979, the FO of *Crenalithus asanoi* ($>6.5 \mu\text{m}$) is recorded above i-cycle 108. Site 977 is selected to calculate the age of this datum because of high sampling resolution, the presence of Sapropels 741 (i-cycle 108) and 740 (i-cycle 100), and a distinct oxygen isotope record. Based on this site, an age of 1.122 Ma is assigned for this datum, which is correlated to i-cycle 106 (at 1.126 Ma). By correlation to the oxygen isotope stratigraphy, this datum occurs at the transition between stages 34 and 33 (Fig. 9).

Datum 8

FO of *Gephyrocapsa omega* ($>4 \mu\text{m}$)

This biohorizon is correlated to the top of the "small *Gephyrocapsa* Zone" of Gartner (1977) and corresponds to the reappearance of medium-sized *Gephyrocapsa*, and especially of *Gephyrocapsa ome-*

ga (>4 µm). According to Matsuoka and Okada (1990), this episode corresponds to the second evolutionary cycle of *Gephyrocapsa* in the Pleistocene and is recognized at its base by the occurrence of *Gephyrocapsa* sp. C, a group of forms with a high bridge angle (>60°), or, in the present study, *Gephyrocapsa omega*. Raffi et al. (1993), using the Shackleton et al.'s (1990) time scale, estimated an age of 1.028 Ma for this biohorizon in the Equatorial Pacific (Site 677) and 0.957 Ma in the North Atlantic (Site 607). Berggren et al. (1995) indicated the re-entrance of medium *Gephyrocapsa* spp. at 1.03 Ma and within oxygen isotope stage 29. Based on the biostratigraphic data from Takayama (1993), Berger et al. (1994) estimated an age of 1.045 Ma (± 0.025) for the FO of *Gephyrocapsa omega* in the western Equatorial Pacific (Site 806). As mentioned above, Berger et al. (1994) used an astronomical time scale calibrated by the solution of Berger and Loutre (1991) to estimate the age of this event. Castradori (1993) estimated an age of 0.944 Ma for the FO of *Gephyrocapsa* sp. 3 and the re-entrance of medium *Gephyrocapsa* (= FO of *Gephyrocapsa omega*) in eastern Mediterranean deep-sea cores.

At Leg 161 sites, the FO of *Gephyrocapsa omega* (>4 µm) is recorded between i-cycle 92 (0.976 Ma) and i-cycle 90 (0.955 Ma). Based on sapropels 621–622 (i-cycle 90) and on oxygen isotope event 26 (at 0.965 Ma) recovered at Site 976 (Fig. 9), an age of 0.962 Ma is assigned for the FO of *Gephyrocapsa omega* (>4 µm). By correlation to the oxygen isotope stratigraphy, this datum is placed at the top of stages 26.

Datum 7

LO of *Crenalithus asanoi* (circular, >6.5 µm)

Different bioevents have been used to define this datum. Takayama and Sato (1987) defined it by the LO of the acme of *Reticulofenestra* sp. A (>6.0), a large subelliptical form. Matsuoka and Okada (1989) used the LO of *Reticulofenestra* sp. A (>6.5 µm) and not the termination of its acme. Sato et al. (1991), Sato and Takayama (1992), and Takayama (1993) all used the LO of *Reticulofenestra asanoi* (>6.0), but they include both subcircular to circular forms in the species concept. Based on the biostratigraphic data from Takayama (1993), Berger et al. (1994) estimated the age of this datum at 0.889 Ma (± 0.025). By correlation, this datum is situated in the oxygen isotope stage 22.

At Leg 161 sites, the LO of *Crenalithus asanoi* (circular; >6.5 µm) is recorded in i-cycle 74 (0.785 Ma). Based on Site 975 (high sampling resolution), an age of 0.781 Ma is assigned to this datum by the oxygen isotope record. An age of 0.781 Ma corresponds to i-cycle 74 and by correlation to the oxygen isotope stratigraphy to the 19.3 event (Fig. 9).

Datum 6

LO acme of *Pseudoemiliana lacunosa*

As illustrated by Matsuoka and Okada (1989), *Pseudoemiliana lacunosa* has much potential as a stratigraphic marker. Changes in size, outline, number of slits in the distal shield, and variations in abundance may be used to zone the Pleistocene with respect to the LO of *Pseudoemiliana lacunosa* (s.s.). We proposed this unconventional acme event to subdivide further the upper Pleistocene interval. This event corresponds to the termination of the acme of *Pseudoemiliana lacunosa* as defined by a decrease in abundance of the *Pseudoemiliana* populations from abundant (1–10 specimens per field of view) to common (1 specimen per 2–10 fields of view). At all Leg 161 sites, we observed a similar decrease in abundance of *Pseudoemiliana* populations above the LO of *Crenalithus asanoi* (>6.5 µm). Matsuoka and Okada (1989) have illustrated in their quantitative analysis of Pleistocene sediments in the western Pacific, that a marked decrease in *Pseudoemiliana* populations occurs about 0.030 Ma above the LO of *Reticulofenestra* sp. A (>6.5 µm).

The top of the acme of *Pseudoemiliana lacunosa* is observed at all Leg 161 sites below i-cycle 68 (0.732 Ma). Because of high sam-

pling resolution, Site 975 is selected to calculate the age of this datum. An age of 0.739 Ma is assigned for the termination of the acme of *Pseudoemiliana lacunosa* by the position of sapropel 518 (i-cycle 68) and by the oxygen isotope event 18.4 (Fig. 9). This age of 0.739 Ma corresponds to i-cycle 69 and, by correlation to the oxygen isotope stratigraphy, to the transition between events 18.4/18.3 (Fig. 9).

Datum 5

LO of *Pseudoemiliana lacunosa lacunosa* (>7.0 µm)

This datum is defined by the extinction of the circular to subcircular variety of *Pseudoemiliana lacunosa* larger than 7 µm (see "Paleontological Systematic Description" below). Several studies have demonstrated the extinction of circular *Pseudoemiliana lacunosa* just before the extinction of elliptical *Pseudoemiliana lacunosa*. A size limit of 7 µm is used herein to define this datum. The ellipticity of medium-sized (5–7 µm) *Pseudoemiliana lacunosa* is difficult to estimate visually. Elliptical and circular *Pseudoemiliana lacunosa* (<5 µm) could not be separated in light microscope analyses.

Hay (1970) remarked that circular forms of *Pseudoemiliana lacunosa* became extinct before the elliptical forms. Matsuoka and Okada (1989) also illustrated, from quantitative morphometric analyses in the subtropical western Pacific, that circular forms of *Pseudoemiliana lacunosa* variety C (with more than 16 slits) disappear about 0.030 m.y. before the LO of elliptical *Pseudoemiliana lacunosa*. They also observed that large elliptical *Pseudoemiliana lacunosa* (>7 µm) disappeared shortly before elliptical forms between 5 and 7 µm.

The same succession of bioevents was also observed in the western Mediterranean. At Site 977 (Fig. 8), *Pseudoemiliana lacunosa lacunosa* (>7 µm) was last observed between i-cycle 40 (at 0.425 Ma) and i-cycle 44 (at 0.461 Ma). Based on oxygen isotope records from Site 976, an age of 0.439 Ma is assigned to this datum and correlates with the i-cycle 41. This datum also corresponds to oxygen isotope event 12.2 (Fig. 9).

Datum 4

LO of *Pseudoemiliana lacunosa*

The LO of *Pseudoemiliana lacunosa* corresponds to the disappearance of elliptical medium-sized forms (between 4–5 µm). Very often, near the top of the stratigraphic range of *Pseudoemiliana lacunosa*, the distal shield elements are malformed (teratological malformation). These malformations do not represent secondary overgrowth, but are primary variations in distal shield elements in late *Pseudoemiliana lacunosa* populations. *Pseudoemiliana lacunosa* forms with teratological malformations have less distinct distal shield slits.

A generally accepted age of 0.458 Ma (Thierstein et al., 1977) is used for the extinction of *Pseudoemiliana lacunosa*, which occurs in the middle of the oxygen isotope stage 12 (about oxygen isotope event 12.33). Different ages have been proposed for this datum. An estimated age of 0.39 Ma is given by Sato and Takayama (1992) in the northeast Atlantic (Site 610). Berger et al. (1994) estimated an age of 0.433 Ma (± 0.020) for the LO of *Pseudoemiliana lacunosa* in the western Equatorial Pacific (Site 806), based on the stratigraphic record of Takayama (1993). They calibrated the nannofossil datum to the astronomical solution developed by Berger and Loutre (1991). Shackleton et al. (1995) estimated an age between 0.344 and 0.749 Ma for the LO of *Pseudoemiliana lacunosa* in the different sites drilled during Leg 138 in the eastern Equatorial Pacific. The age model was also based on the tuning of GRAPE density records.

At Sites 974, 975, 977, and 979, the extinction of *Pseudoemiliana lacunosa* occurs between i-cycle 38 (at 0.405 Ma) and i-cycle 40 (at 0.425 Ma). I-cycle 38 corresponds to the sapropel "S11" in the codification of Cita et al. (1977), and is distinguished at Leg 161 sites by the presence of thick sapropels with relatively high TOC content. Based on Site 975, an age of 0.406 Ma is assigned for the LO of *Pseu-*

doemiliana lacunosa, which corresponds to i-cycle 38. By correlation to the oxygen isotope stratigraphy, this datum is situated in the lower part of oxygen isotope event 11.3.

Datum 3

FO of *Emiliana huxleyi*

The abundance of *Emiliana huxleyi* is extremely low at the base of its stratigraphic range and therefore difficult to find. *Emiliana huxleyi* is a very distinct, small species with a relatively broad distal shield composed of T-shaped elements, a low inner tube, and no bridge. In contrast, *Gephyrocapsa protohuxleyi*, a form abundant at the base of the range of *Emiliana huxleyi*, has a narrow distal shield, a high, broad inner tube, and a central bridge. Misidentification of *Gephyrocapsa protohuxleyi* without bridges (broken center) as *Emiliana huxleyi*, is possible, but unlikely. By examining carefully the distal shield and the inner tube birefringence, these two species can be distinguished with the light microscope.

The generally accepted age for this datum is 0.268 Ma, as calculated by Thierstein et al. (1977). This age corresponds to the oxygen isotope event 8.4 (0.269 Ma). Thierstein et al. (1977) recorded very rare and questionable specimens below this datum level. They correlated the FO of *Emiliana huxleyi* with the lower part of the oxygen isotope stage 8. We compared their oxygen isotope curves with more recent curves and concluded that an age of 0.274 Ma is probably more accurate for the stratigraphic position of the FO of very rare specimens of *Emiliana huxleyi*. Moreover, ages of 0.2735 Ma (Core V22–174) and of 0.274 Ma (Core V19–240) were also estimated by Thierstein et al. (1977) in their table 3. At Sites 974, 975, and 979, the same age of 0.274 Ma (Table 12) is calculated for the FO of very rare specimens of *Emiliana huxleyi*.

At Leg 161 sites, the FO of *Emiliana huxleyi*, based on light microscope analyses, is recorded between i-cycle 24 (at 0.264 Ma) and i-cycle 30 (at 0.331 Ma). Based on oxygen isotope record at Site 976, an age of 0.270 Ma (Table 12) is assigned to this datum, which is correlated to i-cycle 25. This age corresponds to the lower oxygen isotope event 8.4.

Datum 2

FcO (first consistent occurrence) of *Emiliana huxleyi*

This reliable datum is defined by the first consistent occurrence of *Emiliana huxleyi*, which corresponds to approximately one to four specimens counted per mm². At Leg 161 sites, this bioevent is found within the sapropel of i-cycle 20 (at 0.217 Ma). Based on the oxygen isotope record at Site 976, an age of 0.218 Ma (Table 12) is assigned to this datum. By correlation to oxygen isotope stratigraphy, this datum corresponds to oxygen isotope event 7.3. The chronostratigraphic position of this datum is very similar to the lowest occurrence of *Emiliana huxleyi* recorded by Vergnaud-Grazzini et al. (1977) in the eastern Mediterranean. They situated the FO of *Emiliana huxleyi* just above the top of sapropel "S8" (i-cycle 20). The first occurrence of *Emiliana huxleyi* is recorded much earlier in the western Mediterranean. The age difference between the FO of *Emiliana huxleyi* in the eastern and western Mediterranean is probably a result of difficulties in identifying *Emiliana huxleyi* when its abundance is very low and may not indicate a diachronous appearance.

Datum 1

FO *Emiliana huxleyi* > *Gephyrocapsa* spp.

This biohorizon is defined by the dominant occurrence of *Emiliana huxleyi* in the nannofossil assemblage or by the dominance of *Emiliana huxleyi* over *Gephyrocapsa* populations. This datum corresponds to the base of the *Emiliana huxleyi* acme zone of Gartner (1977). Thierstein et al. (1977) showed that the reversal in dominance

from *Gephyrocapsa caribbeanica* to *Emiliana huxleyi* occurs in the oxygen isotope stage 4 (between oxygen isotopic events 4.2 and 5.1) in high latitudes and in the oxygen isotope stage 5a–5b in low latitudes from the North Atlantic.

At Leg 161 sites, this datum occurs between i-cycle 6 (0.055 Ma) and i-cycle 8 (0.081 Ma). Based on the oxygen isotope record at Site 977, an age of 0.070 Ma (Table 12) is estimated for the shift in dominance between *Emiliana huxleyi* and *Gephyrocapsa* spp. An age of 0.070 Ma corresponds to the transition between oxygen isotope stages 4 and 5 (Fig. 9). The same placement of the reversal in dominance from *Gephyrocapsa caribbeanica* to *Emiliana huxleyi* is indicated by Thierstein et al. (1977) in transitional waters and high latitude.

ACKNOWLEDGMENTS

We thank the crew and scientific shipboard party of Leg 161 for their generous collaboration at sea. We acknowledge Rita von Grafenstein, Catherine Pierre, Ralf Tiedemann, and Rainer Zahn for their dedicated effort and for providing isotope data. The authors give many thanks to James Bergen and William Krebs for reviewing part of an early version of this manuscript. This manuscript benefited by thoughtful reviews from Stephan Gartner and Isabella Raffi, and editorial comments from Maria Bianca Cita. Financial support for post-cruise science from the JOI/USSSP to EK is gratefully acknowledged. Thanks are also extended to the postdoctoral support of Dr. S.W. Wise and to the Florida State University.

REFERENCES

- Backman, J., and Shackleton, N.J., 1983. Quantitative biochronology of Pliocene and early Pleistocene calcareous nannofossils from the Atlantic, Indian and Pacific oceans. *Mar. Micropaleontol.*, 8:141–170.
- Berger, A.L., and Loutre, M.F., 1991. Insolation values for the climate of the last 10 million years. *Quat. Sci. Rev.*, 10:297–317.
- Berger, W.H., Yasuda, M.K., Bickert, T., Wefer, G., and Takayama, T., 1994. Quaternary time scale for the Ontong Java Plateau: Milankovitch template for Ocean Drilling Program Site 806. *Geology*, 22:463–467.
- Berggren, W.A., Hilgen, F.J., Langereis, C.G., Kent, D.V., Obradovich, J.D., Raffi, I., Raymo, M.E., and Shackleton, N.J., 1995. Late Neogene chronology: new perspectives in high-resolution stratigraphy. *Geol. Soc. Am. Bull.*, 107:1272–1287.
- Black, M., and Barnes, B., 1961. Coccoliths and discoasters from the floor of the South Atlantic Ocean. *J. R. Microsc. Soc.*, 3/80:137–147.
- Bukry, D., 1973. Coccolith stratigraphy, eastern equatorial Pacific, Leg 16, Deep Sea Drilling Project. In van Andel, T.H., Heath, G.R., et al., *Init. Repts. DSDP*, 16: Washington (U.S. Govt. Printing Office), 653–711.
- Bukry, D., and Bramlette, M.N., 1969. Some new and stratigraphically useful calcareous nannofossils of the Cenozoic. *Tulane Stud. Geol. Paleontol.*, 7:131–142.
- Castradori, D., 1993. Calcareous nannofossil biostratigraphy and biochronology in eastern Mediterranean deep-sea cores. *Riv. Ital. Paleontol. Stratigr.*, 99:107–126.
- Cita, M.B., Vergnaud-Grazzini, C., Robert, C., Chamley, H., Ciaranfi, N., and D'Onofrio, S., 1977. Paleoclimatic record of a long deep sea core from the eastern Mediterranean. *Quat. Res.*, 8:205–235.
- Comas, M.C., Zahn, R., Klaus, A., et al., 1996. *Proc. ODP, Init. Repts.*, 161: College Station, TX (Ocean Drilling Program).
- de Kaenel, E., and Villa, G., 1996. Oligocene-Miocene calcareous nannofossils biostratigraphy and paleoecology from the Iberia Abyssal Plain. In Whitmarsh, R.B., Sawyer, D.S., Klaus, A., and Masson, D.G. (Eds.), *Proc. ODP, Sci. Results*, 149: College Station, TX (Ocean Drilling Program), 79–145.
- Fornaciari, E., Raffi, I., Rio, D., Villa, G., Backman, J., and Olafsson, G., 1990. Quantitative distribution patterns of Oligocene and Miocene calcareous nannofossils from the western equatorial Indian Ocean. In Duncan, R.A., Backman, J., Peterson, L.C., et al., *Proc. ODP, Sci. Results*, 115: College Station, TX (Ocean Drilling Program), 237–254.
- Gartner, S., 1969. Correlation of Neogene planktonic foraminifer and calcareous nannofossil zones. *Trans. Gulf Coast Assoc. Geol. Soc.*, 19:585–599.

- , 1977. Calcareous nannofossil biostratigraphy and revised zonation of the Pleistocene. *Mar. Micropaleontol.*, 2:1–25.
- Hay, W.W., 1970. Calcareous nannofossils from cores recovered on Leg 4. In Bader, R.G., Gerard, R.D., et al., *Init. Repts. DSDP*, 4: Washington (U.S. Govt. Printing Office), 455–501.
- Hilgen, F.J., 1991. Astronomical calibration of Gauss to Matuyama sapropels in the Mediterranean and implication for the geomagnetic polarity time scale. *Earth Planet. Sci. Lett.*, 104:226–244.
- Kamptner, E., 1950. Über den submikroskopischen Aufbau der Coccolithen. *Anz. Österr. Akad. Wiss., Math.-Naturw. Kl.*, 87:152–158.
- , 1963. Coccolithineen-Skelettreste aus Tiefseeablagerungen des Pazifischen Ozeans. *Ann. Naturhist. Mus. Wien*, 66:139–204.
- Laskar, J., Joutel, F., and Boudin, F., 1993. Orbital, precessional, and insolation quantities for the Earth from –20 Myr to +10 Myr. *Astron. Astrophys.*, 270:522–533.
- Loeblich, A.R., and Tappan, H., 1978. The coccolithophorid genus *Calcidiscus* Kamptner and its synonyms. *J. Paleontol.*, 52:1390–1392.
- Lourens, L.J., 1994. Astronomical forcing of mediterranean climate during the last 5.3 million years [Ph.D. thesis]. Univ. Utrecht.
- Lourens, L.J., Antonarakou, A., Hilgen, F.J., Van Hoof, A.A.M., Vergnaud-Grazzini, C., and Zachariasse, W.J., 1996a. Evaluation of the Plio-Pleistocene astronomical timescale. *Paleoceanography*, 11:391–413.
- Lourens, L.J., Hilgen, F.J., Gudjonsson, L., and Zachariasse, W.J., 1992. Late Pliocene to early Pleistocene astronomically forced sea surface productivity and temperature variations in the Mediterranean. *Mar. Micropaleontol.*, 19:49–78.
- Lourens, L.J., Hilgen, F.J., Raffi, I., 1998. Base of large *Gephyrocapsa* and astronomical calibration of early Pleistocene sapropels in Site 967 and Hole 969D: solving the chronology of the Vrica section (Calabria, Italy). In Robertson, A.H.F., Emeis, K.-C., Richter, C., and Camerlenghi, A. (Eds.), *Proc. ODP, Sci. Results*, 160: College Station, TX (Ocean Drilling Program), 191–197.
- Lourens, L.J., Hilgen, F.J., Raffi, I., and Vergnaud-Grazzini, C., 1996b. Early Pleistocene chronology of the Vrica section (Calabria, Italy). *Paleoceanography*, 11:797–812.
- Martini, E., 1971. Standard Tertiary and Quaternary calcareous nannoplankton zonation. In Farinacci, A. (Ed.), *Proc. 2nd Int. Conf. Planktonic Microfossils Roma*: Rome (Ed. Tecnosci.), 2:739–785.
- Matsuoka, H., and Okada, H., 1989. Quantitative analysis of Quaternary nannoplankton in the subtropical northwestern Pacific Ocean. *Mar. Micropaleontol.*, 14:97–118.
- , 1990. Time-progressive morphometric changes of the genus *Gephyrocapsa* in the Quaternary sequence of the tropical Indian Ocean, Site 709. In Duncan, R.A., Backman, J., Peterson, L.C., et al., *Proc. ODP, Sci. Results*, 115: College Station, TX (Ocean Drilling Program), 255–270.
- Murat, A., 1991. Enregistrement sédimentaire des paléoenvironnements Quaternaires en Méditerranée Orientale [Ph.D. dissert.]. University of Perpignan, France.
- Raffi, I., Backman, J., Rio, D., and Shackleton, N.J., 1993. Plio-Pleistocene nannofossil biostratigraphy and calibration to oxygen isotopes stratigraphies from Deep Sea Drilling Project Site 607 and Ocean Drilling Program Site 677. *Paleoceanography*, 8:387–408.
- Raffi, I., and Flores, J.-A., 1995. Pleistocene through Miocene calcareous nannofossils from eastern equatorial Pacific Ocean (Leg 138). In Pisias, N.G., Mayer, L.A., Janecek, T.R., Palmer-Julson, A., and van Andel, T.H. (Eds.), *Proc. ODP, Sci. Results*, 138: College Station, TX (Ocean Drilling Program), 233–286.
- Rio, D., 1982. The fossil distribution of coccolithophore genus *Gephyrocapsa* Kamptner and related Plio-Pleistocene chronostratigraphic problems. In Prell, W.L., Gardner, J.V., et al., *Init. Repts. DSDP*, 68: Washington (U.S. Govt. Printing Office), 325–343.
- Rio, D., Fornaciari, E., and Raffi, I., 1990a. Late Oligocene through early Pleistocene calcareous nannofossils from western equatorial Indian Ocean (Leg 115). In Duncan, R.A., Backman, J., Peterson, L.C., et al., *Proc. ODP, Sci. Results*, 115: College Station, TX (Ocean Drilling Program), 175–235.
- Rio, D., Raffi, I., Backman, J., 1997. Calcareous nannofossil biochronology and the Pliocene/Pleistocene boundary: the Neogene/Quaternary boundary. In Van Couvering, J.A. (Ed.), *The Pleistocene Boundary and the Beginning of the Quaternary: Final Report of the International Geological Correlation Program-Project 41, Neogene-Quaternary Boundary*: Cambridge (Cambridge Univ. Press), 63–78.
- Rio, D., Raffi, I., and Villa, G., 1990b. Pliocene-Pleistocene calcareous nannofossil distribution patterns in the Western Mediterranean. In Kastens, K.A., Mascle, J., et al., *Proc. ODP, Sci. Results*, 107: College Station, TX (Ocean Drilling Program), 513–533.
- Rio, D., Sprovieri, R., and Thunell, R., 1991. Pliocene–lower Pleistocene chronostratigraphy: a re-evaluation of Mediterranean type sections. *Geol. Soc. Am. Bull.*, 103:1049–1058.
- Roth, P.H., 1973. Calcareous nannofossils—Leg 17, Deep Sea Drilling Project. In Winterer, E.L., Ewing, J.I., et al., *Init. Repts. DSDP*, 17: Washington (U.S. Govt. Printing Office), 695–795.
- Sato, T., Kameo, K., and Takayama, T., 1991. Coccolith biostratigraphy of the Arabian Sea. In Prell, W.L., Niitsuma, N., et al., *Proc. ODP, Sci. Results*, 117: College Station, TX (Ocean Drilling Program), 37–54.
- Sato, T., and Takayama, T., 1992. A stratigraphically significant new species of the calcareous nannofossil *Reticulofenestra asanoi*. In Ishizaki, K., and Saito, T. (Eds.), *Centenary of Japanese Micropaleontology*: Tokyo (Terra Sci. Publ.), 457–460.
- Shackleton, N.J., Baldauf, J.G., Flores, J.-A., Iwai, M., Moore, T.C. Jr., Raffi, I., and Vincent, E., 1995. Biostratigraphic summary for Leg 138. In Pisias, N.G., Mayer, L.A., Janecek, T.R., Palmer-Julson, A., and van Andel, T.H. (Eds.), *Proc. ODP, Sci. Results*, 138: College Station, TX (Ocean Drilling Program), 517–536.
- Shackleton, N.J., Berger, A., and Peltier, W.A., 1990. An alternative astronomical calibration of the lower Pleistocene timescale based on ODP Site 677. *Trans. R. Soc. Edinburgh: Earth Sci.*, 81:251–261.
- Sprovieri, R., 1993a. Astrochronology of Pliocene-early Pleistocene Mediterranean calcareous plankton events. *Paleopelagos*, 3:187–194.
- , 1993b. Pliocene–early Pleistocene astronomically forced planktonic foraminifera abundance fluctuations and chronology of Mediterranean calcareous plankton bio-events. *Riv. Ital. Paleontol. Stratigr.*, 99:371–414.
- Takayama, T., 1993. Notes on Neogene calcareous nannofossil biostratigraphy of the Ontong Java Plateau and size variations of *Reticulofenestra* coccoliths. In Berger, W.H., Kroenke, L.W., Mayer, L.A., et al., *Proc. ODP, Sci. Results*, 130: College Station, TX (Ocean Drilling Program), 179–229.
- Takayama, T., and Sato, T., 1987. Coccolith biostratigraphy of the North Atlantic Ocean, Deep Sea Drilling Project Leg 94. In Ruddiman, W.F., Kidd, R.B., Thomas, E., et al., *Init. Repts. DSDP*, 94 (Pt. 2): Washington (U.S. Govt. Printing Office), 651–702.
- Thierstein, H.R., Geitzenauer, K., Molino, B., and Shackleton, N.J., 1977. Global synchronicity of late Quaternary coccolith datum levels: validation by oxygen isotopes. *Geology*, 5:400–404.
- Vergnaud-Grazzini, C., Ryan, W.B.F., and Cita, M.B., 1977. Stable isotope fractionation, climatic change and episodic stagnation in the Eastern Mediterranean during the Late Quaternary. *Mar. Micropaleontol.*, 2:353–370.
- Young, J.R., 1990. Size variation of Neogene *Reticulofenestra* coccoliths from Indian Ocean DSDP cores. *J. Micropaleontol.*, 9:71–85.
- Young, J.R., Bergen, J.A., Bown, P.R., Burnett, J.A., Fiorentino, A., Jordan, R.W., Kleijne, A., van Niel, B.E., Ton Romein, A.J., von Salis, K., 1997. Guidelines for coccolith and calcareous nannofossil terminology. *Paleontology*, 40:875–912.

Date of initial receipt: 3 June 1997

Date of acceptance: 16 February 1998

Ms 161SR-250

APPENDIX A

Paleontological Systematic Description

Genus *Calcidiscus* Kamptner, 1950

Calcidiscus macintyre (Bukry and Bramlette, 1969) Loeblich and Tappan, 1978
(Pl. 1, figs. 23–28)

Remarks: Variations in size, shape, and central area features are used to differentiate *Calcidiscus* species. Circular to elliptical paololiths have been observed. Large (>11 µm), circular specimens of *Calcidiscus*, with more than 40 distal elements, occur in the lowermost Pleistocene interval. These forms have

variable central area features, being closed or with a central opening. Circular forms with a large central opening are grouped into *Calcidiscus tropicus*. Circular forms larger than 11 µm, with a closed central area or with a small central opening, are grouped into *Calcidiscus macintyreii*.

Close to the LO of circular *Calcidiscus* spp. (>11 µm), another group of large, subelliptical to elliptical forms first occur. These large (>11 µm), non-circular specimens (Pl. 1, figs. 21, 22) have fewer and larger distal elements and a closed central area. This morphogroup of *Calcidiscus leptoporus* (Pl. 1, figs. 21, 22) becomes extinct in the middle Pleistocene, much later than the circular forms. The last occurrence of circular *Calcidiscus* spp. larger than 11 µm and with more than 40 elements occurs in the lower Pleistocene (datum 17). Specimens of circular *Calcidiscus* spp. between 10 and 11 µm are found with *Gephyrocapsa* spp. (>5 µm). In our study, the LO of *Calcidiscus macintyreii* datum is based on circular forms larger than 11 µm.

Genus *Crenalithus* Roth, 1973 emend.

Type species: *Crenalithus doronocoides* (Black and Barnes, 1961) Roth, 1973.

Emended diagnosis: Circular to elliptical Reticulofenestraceae constructed of two bicyclic shields. The distal shield is composed of an outer cycle, which may have up to four slits, and of an inner cycle that may protrude distally.

Discussion: The genus *Crenalithus* first occurs in the late Miocene (NN11) with *Crenalithus sessilis* and *Crenalithus doronocoides*. The genus *Pseudoemiliana* has a first occurrence in the early Pliocene (NN15) with *Pseudoemiliana lacunosa ovata*. In the Pliocene and Pleistocene interval, there are three distinctly different assemblages in the reticulofenestrid group: (1) the genus *Crenalithus* introduced by Roth (1973) is emended here to group reticulofenestrids, which have up to four slits in the distal shield; (2) reticulofenestrids with more than 4 slits are grouped in the genus *Pseudoemiliana*; (3) reticulofenestrids without slits are grouped into the genus *Reticulofenestra*. Some specimens of *Crenalithus doronocoides* and *Crenalithus asanoi* may have a distal shield without slits. These forms may be distinguished from *Reticulofenestra* by their extinction pattern; the outer distal cycle is non-birefringent, or faintly birefringent, and no distinct extinction lines separate the outer and the inner distal cycle (gephyrocapsid extinction pattern).

Crenalithus asanoi (Sato and Takayama, 1992) n. comb.
(Pl. 1, figs. 8–10)

1989 *Reticulofenestra* sp. A (>6.5 µm), Matsuoka and Okada, p. 103, plate 1, figures 25, 28.

1992 *Reticulofenestra asanoi* Sato and Takayama, p. 458, figures 3–7 to 3–14.

Emended diagnosis: A medium to large, subcircular to circular species of *Crenalithus* with up to 4 slits in the outer distal cycle and a wide inner distal cycle.

Size: >6.5 µm; maximum size observed 12 µm (holotype: 6.85 µm).

Discussion: Sato and Takayama (1992) also distinguished *Crenalithus asanoi* from *Crenalithus doronocoides* by its larger size and circular to subcircular outline. *Crenalithus* species are separated according to the size. Small forms up to 3 µm are grouped in the species *Crenalithus sessilis*, forms larger than 3 µm up to 5 µm are grouped in the species *Crenalithus doronocoides*, and

forms larger than 5 µm up to 6.5 µm are grouped in the species *Crenalithus japonicus*.

Crenalithus japonicus (Nishida, 1971 emend. Nishida, 1979) n. comb.
(Pl. 1, fig. 4 [upper specimen], figs. 5–7)

1971 *Gephyrocapsa reticulata* Nishida; p. 150–151, plate 17, figures 1–3, text figure 1.

1979 *Reticulofenestra japonica* (Nishida, 1971) emend. Nishida (non. substit. pro *G. reticulata*); p. 105, plate 1, figures 1–3.

Emended diagnosis: A medium-sized, subcircular to circular species of *Crenalithus* with up to 4 slits in the outer distal cycle and a wide inner distal cycle.
Size: >5–6.5 µm.

Crenalithus doronocoides (Black and Burns, 1961) Roth, 1973
(Pl. 1, figs. 1–3, fig. 4 [lower specimen])

Genus *Pseudoemiliana* Gartner, 1969

Pseudoemiliana lacunosa (Gartner, 1969, ex Kamptner, 1963) var. *lacunosa*
(Young 1990) n. comb.
(Pl. 1, figs. 16–20)

1963 *Ellipsoplacolithus lacunosus* Kamptner; p. 172, plate 9, figure 50.

1969 *Pseudoemiliana lacunosa* (Kamptner) Gartner; p. 598, plate 2, figures 9–10.

1990 *Reticulofenestra lacunosa* (Gartner, 1969, ex Kamptner, 1963) *lacunosa*
Young; p. 83.

Emended diagnosis: Circular to subcircular variety of *Pseudoemiliana lacunosa* with more than twelve slits in the distal shield.

Size: 4 to 10 µm.

Pseudoemiliana lacunosa var. *ovata* (Young, 1990) n. comb.
(Pl. 1, figs. 11, 12)

1973 *Emiliana ovata* Bukry; p. 678, plate 2, figures 10–12.

non 1979 *Reticulofenestra pacifica* Nishida; p. 106, plate 1, figures 4–6.

1990 *Reticulofenestra lacunosa ovata* (Young, 1990); p. 83.

Emended diagnosis: A small- to medium-sized, elliptical variety of *Pseudoemiliana lacunosa* with less than twelve slits in the distal shield.

Size: 4 to 6.5 µm; specimens larger than 6.5 µm are grouped into the species *Pseudoemiliana pacifica*.

Pseudoemiliana pacifica (Nishida, 1979) n. comb.
(Pl. 1, figs. 13–15)

1979 *Reticulofenestra pacifica* Nishida; p. 106, plate 1, figures 4–6.

Emended diagnosis: A medium-sized, elliptical *Pseudoemiliana* with less than twelve slits in the distal shield.

Size: >6.5 µm.

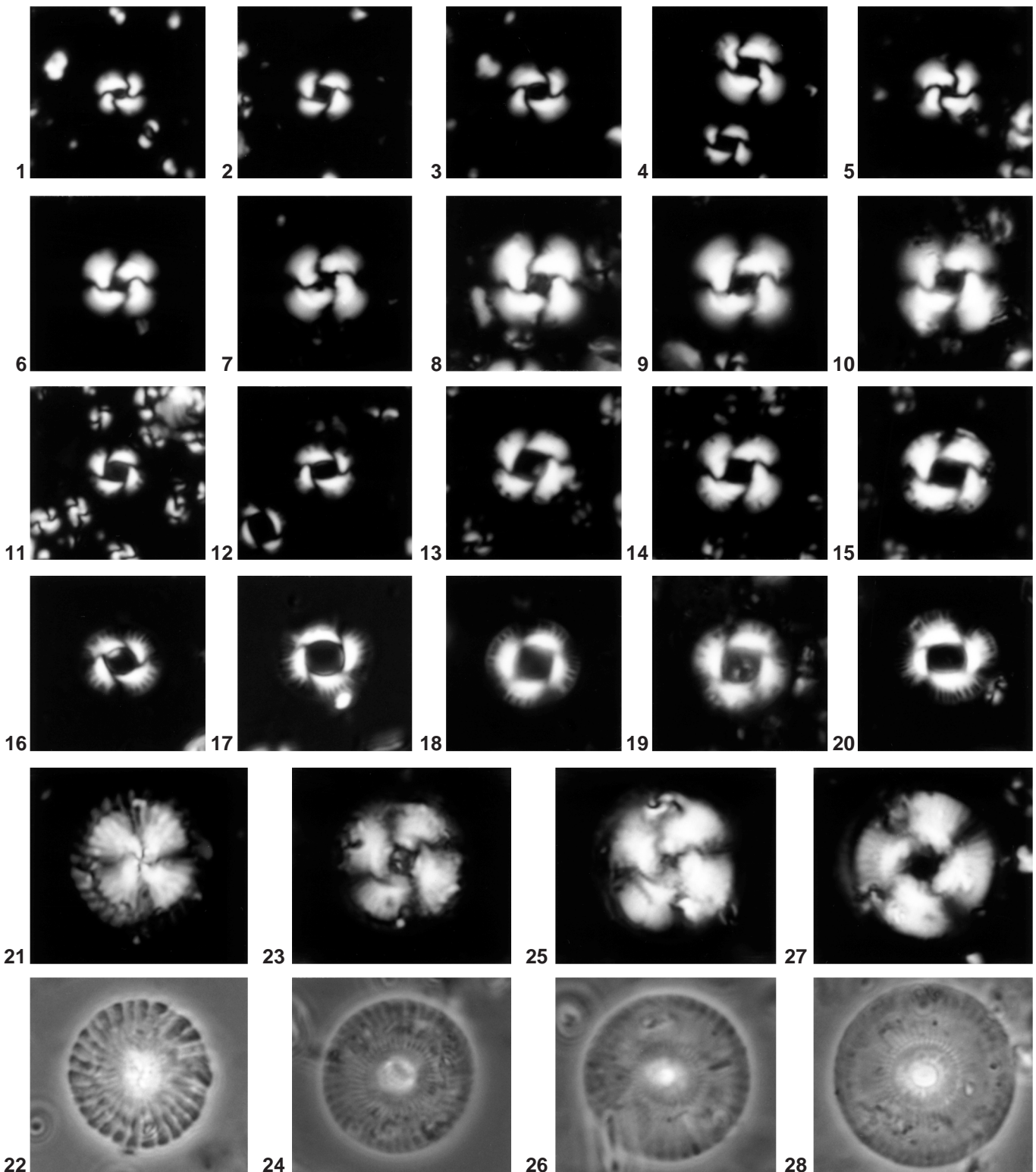


Plate 1. Magnification for all specimens is 2500 \times . XP = cross-polarized ligh, Ph = phase contrast. **1–3.** *Crenalithus doronocoides* (Black and Burns) Roth, Sample 161-975B-14H-5, 82–84 cm, XP. **4.** Lower specimen, *Crenalithus doronocoides* (Black and Burns) Roth; upper specimen *Crenalithus japonicus* (Nishida emend. Nishida) n. comb., Sample 161-975B-9H-3, 88–90 cm, XP. **5–7.** *Crenalithus japonicus* (Nishida emend. Nishida) n. comb. (5) Sample 161-976B-26X-3, 73–75 cm, XP. (6) Sample 161-975B-8H-2, 99–101 cm, XP. (7) Sample 161-976B-26X-3, 73–75 cm, XP. **8–10.** *Crenalithus asanoi* (Sato and Takayama) n. comb., Sample 161-975B-8H-5, 137–138 cm, XP. **11–12.** *Pseudoemiliana lacunosa ovata* (Young) n. comb. (11) Sample 161-974B-6H-5, 110–112 cm, XP. (12) Sample 161-975B-14H-5, 82–84 cm, XP. **13–15.** *Pseudoemiliana pacifica* (Nishida) n. comb., Sample 161-974B-6H-5, 110–112 cm, XP. **16–20.** *Pseudoemiliana lacunosa* (Gartner ex Kamptner) *lacunosa* (Young) n. comb. (16–18, 20) Sample 161-975B-8H-2, 99–101 cm, XP. (19) Sample 161-975B-8H-5, 137–138 cm, XP. **21–22.** *Calcidiscus leptoporus* (Murray and Blackman) Loeblich and Tappan, (>11 μ m, elliptical), Sample 161-975B-13H-3, 90–91 cm, XP (21) and Ph (22). **23–28.** *Calcidiscus macintyreii* (Bukry and Bramlette) Loeblich and Tappan, (>11 μ m, circular). (23–24) Sample 161-975B-13H-4, 110–111 cm, XP (23) and Ph (24). (25–28) Sample 161-975B-13H-6, 45–46 cm. (25–26) XP and Ph. (27–28) XP and Ph.